# INVESTIGATING THE COMPATIBILITY OF BIODIESEL ON POLYETHYLENE

# INVESTIGATING THE COMPATIBILITY OF BIODIESEL ON POLYETHYLENE THROUGH NONDESTRUCTIVE AND TRADITIONAL METHODS

By: AHMED K. SAAD, B. Eng.

A Thesis Submitted to the School of Graduate Studies in Partial Fulfillment of the
Requirements for the Degree Master of Applied Science

McMaster University MASTER OF APPLIED SCIENCE (2019) Hamilton, Ontario (Chemical Engineering)

TITLE: Investigating The Compatibility of Biodiesel On Polyethylene Through Nondestructive and Traditional Methods

AUTHOR: Ahmed K. Saad, B.Eng. (McMaster University)

SUPERVISORS: Professor Dr. Michael R. Thompson, Professor Emeritus Dr. John Vlachopoulos

NUMBER OF PAGES: xviii, 126

# Lay Abstract

Understanding the compatibility of polymers with chemicals that they are exposed to is essential, particularly those used for liquid storage components like fuel tanks, making it vital to consider both short-term and long-term interactions under environmental conditions that regularly fluctuate. A two-stage project based on experimental trials has been conducted, using traditional testing methods and a novel non-destructive testing method based on ultrasonics, to evaluate the compatibility of biodiesel with different grades of Imperial Oil ltd. polyethylenes. In the first stage of the study, the plasticization effect of fresh and degraded biodiesel (in comparison to toluene) was investigated on polyethylene. Results were used in the second stage of this experiment to propose a plasticization mechanism targeting tie molecules as the proposed pathway for environmental stress cracking of biodiesel with polyethylene.

# Abstract

Being the most abundant cause of unexpected brittle failures of polymers, environmental stress cracking (ESC) is a major issue for the plastics industry, accounting for approximately 15-40% of all plastic part failures in service. ESC is an intriguing phenomenon that is not yet well understood, which relates to the accelerated failure of a stressed polymer whilst the presence of an active medium, such as biodiesel. Unexpected failures of polyethylene parts in tanks aboard marine vessels that were operated with biodiesel has generated concerns in the polymer industry over the compatibility of this relatively new fuel, making investigations into these failures both urgent and essential for the process of change towards renewable fuel standards.

Experimental trials carried out for a two-stage project investigating the compatibility of fresh and degraded biodiesel with polyethylene were used to suggest a plasticization mechanism targeting tie molecules (often related to micellular contaminants in a contacting medium) as the probable pathway for ESC of polyethylene with biodiesel. Preliminary analysis was done using the Bell Test (ASTM D1693) showing evidence of pure biodiesel as a stress cracking agent with an aggressiveness similar to a 10% biodiesel in water solution for which the majority of trials used.

Results from the first stage of this study revealed evidence of differing modes of interaction for biodiesel and toluene (a known plasticizing agent) with the semi-crystalline polymer structure. The second stage utilized acoustic analysis to monitor internal stresses during long-term aging to better explain the theory of ESC for

polyethylene with biodiesel, showing that both plasticization and ESC behaviors occurred.

# Acknowledgements

I would like to express my sincere appreciation and gratitude to everyone who has helped me develop this thesis. Firstly, I would like to thank Imperial Oil Ltd. and the Natural Sciences and Engineering Research Council (NSERC) for funding the work. I would also like to thank Ron Cooke at Imperial Oil for his supply of materials and very helpful advice and technical insights.

I cannot express my deep appreciation to my supervisor, Dr. Michael Thompson, who has supported, trusted, and taught me a lot during the past 24 months. This thesis would have not been possible without his help and guidance. I would also like to thank my co-supervisor, Dr. John Vlachopoulos, for his helpful insights during our meetings.

I would also like to express my gratitude to Felipe Gomes and Hassan Abdulhussain who collaborated with me on my first and second papers, respectively. Felipe's guidance and help is one of the main reasons behind the completion of this thesis and Hassan's immense help and encouragement on the second paper has made it possible. I am also grateful to Heera Maraway for his time training me on all the instruments, his help with several tests, and his frequent advice. I would also like to mention the importance of my colleagues: Tomislav Ivanvic, JinLei Li, and Vladimir Gritsichine at the university for their help whenever needed.

Finally, this would have not been possible without the invaluable support and encouragement from my parents, Khaled Saad and Nehal Issa, and my brothers, Marwan

Saad and Yousef Saad. I owe them all the gratitude and appreciation in the world as none of this would have been possible without them.

# Table of Contents

# List of Figures

# List of Tables

# List of Abbreviations and Symbols

**ESC:** Environmental Stress Cracking

**SCG:** Slow Crack Growth

**ESCR:** Environmental Stress Cracking Resistance

**TMs:** Tie Molecules

**HDPE:** High Density Polyethylene

**LLDPE:** Linear Low Density Polyethylene

**LDPE:** Low Density Polyethylene

**PE:** Polyethylene

**MWD:** Molecular Weight Distribution

**NCTL:** Notched Constant Tensile Load Test

**PENT:** Pennsylvania Notch Test

**UV-VIS:** Ultraviolet-Visible Spectroscopy

**FT-IR:** Fourier Transform Infrared Spectroscopy

**ATR:** Attenuated Total Reflection

**$M_t$:** Mass Uptake of Biodiesel into the Polyethylene Slab up to Time t

**$M_\infty$:** Equilibrium Mass Uptake

**D**: Diffusivity Coefficient

**l:** Thickness of the Slab

**$EM_0$:** Original Modulus of the Polymer in the Absence of a Plasticizer

**EM:** Modulus of the Polymer after Immersion in a Plasticizer

**$k_{EM}$:** Plasticizing Efficiency of a Penetrant

**x:** Plasticizer Content

**$A_3$:** Third Harmonic Region between 400-500 kHz

**$A_1$:** Primary Input Frequency between 135-165 kHz

**DSC:** Differential Scanning Calorimetry

**% Crystallinity:** Percent Crystallinity

**$\Delta \mathbf{H}_{\mathbf{f}_{\mathbf{sample}}}$:** Enthalpy of Fusion of the Sample

**$\Delta \mathbf{H}_{\mathbf{f}_{\mathbf{100\%\ crystalline\ PE}}}$:** Enthalpy of fusion for a 100% crystalline PE

# Declaration of Academic Achievements

In accordance with the guidelines for the preparation of a Master of Applied Science thesis set forth by the McMaster University School of Graduate Studies, this work has been prepared as a sandwich thesis. The majority of the work described in this thesis was conducted, interpreted, and written by the author of this thesis. The work was done in consultation with and under the supervision of Dr. Michael R. Thompson and Dr. John Vlachopoulos who also revised the drafts to the final versions. An outline of the contributions of the authors, other than myself and my supervisors are indicated at the opening statement of each chapter.

# Chapter

# 1. Introduction

The use of polymers in the design of parts involving contact with chemicals always comes with a routine concern: compatibility. Compatibility assessment refers to the identification of chemical and physical interactions that would undermine the functionality of parts manufactured with a polymer, in this case polyethylene. Polyethylene (PE) is a leading and popular material in present industries, with several versatile properties that allows it to be used for several domestic and industrial applications. These uses include chemical storage for fuel tanks in automobiles, marine vessels, and agricultural machinery [1].

Biodiesel, a promising petrol alternative for diesel engines, is derived from sustainable feedstocks such as vegetable oils and/or animal renderings. It has been an attractive area for research studies due to its ability of offering greater security to a nation's energy needs while reducing carbon monoxide and hydrocarbon emissions. It is currently being blended at low fractions (less than 10 wt%) with more traditional fossil fuels for the transportation industry and at much higher fractions in marine vessels and agricultural farm equipment. The polymer industry has rising concerns over the compatibility of this new fuel with current tank construction (being primarily fabricated with PE) as a result of some unexplained tank failures in marine vessels operated with biodiesel. Being a bio-sourced fuel alternative to fossil fuels of such importance to the environment and the economy, the increased use of biodiesel is essential to meet the set standards of the Renewable Fuels Strategy in order to proceed towards reducing Canada's total greenhouse gas emissions. This makes investigation into the compatibility of biodiesel with PE of vital importance.

With long-term compatibility studies finding no linkage to chemical and biological degradative reasons for PE failures in the presence of biodiesel [2-6], attention in this work turned to environmental stress cracking (ESC). ESC has been the primary and most common cause of unexpected brittle failures of polymers in parts while in service, making it a theory of significant importance that is not yet well understood and requires intensive consideration. It is an interesting phenomenon where long term physical damage occurs while in contact with a seemingly inert/compatible fluid that accelerates failures in the presence of minor stresses that should be readily tolerated. In light of biodiesel's possible ability to accelerate those tank failures, ESC seems reasonable as the viable cause.

To investigate, a project involving two stages of experimental trials studied the compatibility of fresh and degraded (oxidized) biodiesel with PE. The work employed traditional testing methods (i.e. Bell Test) and a novel nondestructive testing method based on ultrasonics. The goals were to evaluate biodiesel's plasticization ability (in comparison to toluene) as well as its ESC ability at the macro- and meso-scale for different grades of Imperial Oil ltd. PEs.

The published paper presented in Chapter Three, depicts results from the first stage of the study, focused on the plasticization. Gravimetric analysis of biodiesel absorption into different grades of PE revealed higher penetration in lower density (i.e. lower crystallinity) PE grades, based on calculated diffusivity coefficients. A decline in the mechanical properties of the samples confirmed the plasticizing nature of biodiesel on PE. Ultrasonic testing of biodiesel and toluene plasticized samples revealed their differing modes of interaction on the semi-crystalline polymer structure. Included in the first stage of the study was an assessment of the plasticizing ability of PE by a degraded biodiesel in comparison to a nondegraded, which was done in recognition to the unstable chemical nature of this fuel. With degraded biodiesel, a slightly lower diffusion rate was found into PE due to its more hydrophilic nature, but the effects of this absorbed fuel (at equivalent content) in PE showed no significant differences on acoustic or mechanical properties otherwise.

The drafted manuscript presented in Chapter Four, presents the results from the second stage of the study, which focused on the ESC property. Using the Bell Test (ASTM D1693), pure biodiesel showed evidence as a stress cracking agent with an aggressiveness similar to a 10% biodiesel in water solution. Gravimetric analysis, Fourier-transform infrared spectroscopy (FT-IR), microscopic imaging, and visual inspection were used to explain the results from the Bell Test of different PE grades. The novel ultrasonic testing method was applied to monitor internal stresses in the polymer during ESC. The different acoustic signatures (aka spectral fingerprints) attained through ultrasonic testing showed failure was a result of events that could be described as plasticization and stress cracking. The findings helped propose a plasticization contribution to the probable pathway for ESC of PE with biodiesel.

## References

[1] O.-G. Piringer, A.L. Baner, Plastic packaging: interactions with food and pharmaceuticals, Wiley-VCH, Weinheim, 2008.

[2] M. Thompson, B. Mu, C. Ewaschuk, Y. Cai, K. Oxby, J. Vlachopoulos, Long term storage of biodiesel/petrol diesel blends in polyethylene fuel tanks, Fuel. 108 (2013) 771–779. doi:10.1016/j.fuel.2013.02.040.

[3] A. Saad, F. Gomes, M. Thompson, Plasticizing effect of oxidized biodiesel on polyethylene observed by nondestructive method, Fuel. 252 (2019) 246–253. doi:10.1016/j.fuel.2019.04.122.

[4] J.-M. Restrepo-Flórez, A. Bassi, L. Rehmann, M.R. Thompson, Investigation of biofilm formation on polyethylene in a diesel/biodiesel fuel storage environment, Fuel. 128 (2014) 240–247. doi:10.1016/j.fuel.2014.02.052.

[5] J.-M. Restrepo-Flórez, A. Bassi, L. Rehmann, M.R. Thompson, Effect of biodiesel addition on microbial community structure in a simulated fuel storage system, Bioresource Technology. 147 (2013) 456–463. doi:10.1016/j.biortech.2013.08.068.

[6] J.-M. Restrepo-Flórez, A. Bassi, M.R. Thompson, Microbial degradation and deterioration of polyethylene – A review, International Biodeterioration & Biodegradation. 88 (2014) 83–90. doi:10.1016/j.ibiod.2013.12.014.

# Chapter

# 2. Literature Review

The following chapter presents the definitions of basic concepts and recent important publications of the main areas related to the research that influenced the findings present in the subsequent chapters.

## 2.1. Biodiesel and its compatibility with polyethylene

As the population grows, lifestyle requirements increase and so does the use of various energy sources. Many energy sources today rely upon fossil fuels, such as petroleum, and natural gas. They are considered as non-renewable sources, meaning that they are being depleted faster than they are being created. The predicted shortage of fossil fuels has directed research towards nations finding substitutes that meet their rising energy demands and compensate for diminishing petroleum reserves, which has ultimately led to several viable bio-sourced fuels including biodiesel [1].

The term “biodiesel” is generally referring to any diesel fuel substitute that is derived from renewable mass. It is non-toxic, contains no aromatics, has higher degradability than fossil diesel, is less polluting to water and soil, and does not contain sulphur, all which are seen as environmentally beneficial [2]. Over a century ago, Rudolf Diesel tested vegetable oil as a fuel for his engine, and in the 1930s and 1940s vegetable oils were used for diesel fuels from time to time until petroleum-derived sources became available. Those petroleum sources ultimately led to the displacement of biofuels primarily due to problems that rose from the use of vegetable oils in engines that have been optimized to run on petroleum derivatives and not vegetable oils [2]. With a growing scarcity of petroleum-based fuels in the new century, interest has been renewed through research and commercialization activities. Currently, the miscibility of biodiesel with Petro-diesel has led to it being blended at low fractions (less than 10 wt%) into fuels for the transportation industry and at higher fractions in marine vessels and agricultural farm equipment [3]. Unfortunately, several issues have evolved that have slowed down its increased use for transportation, one of which has been its compatibility with PE, a major material in fuel tank fabrication. With regulatory drivers recommending the increased use of biodiesel to shift dependency away from fossil fuel reserves, intense research must go into understanding the compatibility of biodiesel with commonly employed materials.

Biodiesel is a fatty acid methyl ester (FAME) that is derived from a variety of sustainable feedstocks, such as vegetable oils (soybean, cottonseed, palm, peanut, rapeseed, etc.), waste oils (used frying oils), and animal fats (usually tallow) [3]. The biodiesel used in this study was a pure tallow-based methyl ester prepared from animal renderings through a catalyzed transesterification reaction. In this process, monoalkyl esters are formed by a reaction between the triglycerides in the animal fat with a simple monohydric alcohol (usually methanol), in the presence of a catalyst (usually a strong base such as sodium or potassium hydroxide) [4].

Most research centered on biodiesel has been focused on its synthesis and properties with only a small portion focusing on its compatibility with the fuel system components of different transportation systems. Fuels tanks are now fabricated primarily from PE (with other resins like polyamides for barrier layers) and a few recent studies [5-12] on its compatibility with biodiesel have suggested that there are interactions between the two, making the understanding of their compatibility a matter of great importance for the use of biodiesel as a fuel alternative to fossil fuels. Compatibility studies on biodiesel with polymers other than PE, elastomers for example, have reported swelling with a decline in mechanical properties upon exposure to biodiesel [13, 14]. A limited number of long-term compatibility studies [5, 8-10, 12, 15] of biodiesel with high density polyethylene (HDPE) have conveyed swelling with notable weight gains and discoloration of the polymer; with a few of them [9-11, 15] reporting a plasticization nature for biodiesel. In the presence of some chemical affinity between biodiesel (solvent) and the polymer (solute), the increase in volume or swelling resulted as the extent of liquid absorption exceeded the extent of extraction. In other words, the solvent material that is not solubilized by the polymer is retained within causing an increase in the polymer's volume. Plasticization has been evident by the reduced Young's Modulus and increasing strain at max stress as the concentration of absorbed fuel in the polymer increased [15]. Related research [16-22] have shown fatty acids and vegetable oils to be effective plasticizing agents in several polymeric materials and rubbers.

Aside from the plasticization effects of biodiesel on PE, a couple of recent compatibility studies [7, 15] of biodiesel with PE have suggested that biodiesel is an environmental stress cracking agent for PE, resulting in the premature failure of service parts manufactured from the polymer. Studies on their compatibility revealed no chemical degradative interactions, and in the presence of water a small possibility of biodegradative interaction [12, 22].

Long-term durability studies [12, 15, 23, 24] of biodiesel storage have found the fuel itself to be susceptible to degradation by oxidation. The oxidative and thermal sensitivity of biodiesel are important properties affecting its stability during extended storage and both are dependent on a multitude of factors including its feedstock source, the production method, impurities and fuel additives, and the storage and handling methods [25]. Oxidative instability may lead to the formation of by-products such as fatty acids, alcohols, and aldehydes. These by-products are often tracked by the measurement of the peroxide value for hydroperoxides, or acid number for the formation of fatty acids. The resistance of biodiesel to oxidation is lower than petroleum diesel, particularly due to the absence of sulphur in the former case [25]. Thermal instability is implied by an increase in weight of the fluid due to higher oxidation rates at elevated temperatures [26]. A few year-long studies on the stability of biodiesel [8, 12] have reported no chemical effect of biodiesel degradation on PE over time, while others [10, 11, 27, 28] have correlated the formation of unsaturated fatty acids during aging with accelerated oxidative degradation in the PE. The dissimilarity in the results could be attributed to the different testing conditions used in the studies.

The compatibility of biodiesel with PE is still an open issue that is not yet well understood and requires more intensive research for their safe use and in order to satisfy the compatibility concerns brought about by the industry.

## 2.2. Environmental stress cracking

The loss of inherent mechanical properties upon exposure to adverse environments is one of the major shortcomings of polymeric materials. A particular problem is the premature cracking of stressed glassy polymers (mostly crystalline polymers like PE) upon exposure to specific organic liquids. The stress required for failure in the presence of these organic liquids is usually an order of magnitude lower than the actual tensile strength of the polymer [29]. These failures can be traced to a phenomenon known as environmental stress cracking (ESC), which is described by Wright as: “Assisted cracking” or “The premature initiation of cracking and embrittlement of a plastic due to the simultaneous action of stress and strain and contact with specific fluids” [30].

ESC, which accounts for approximately 15-40% of all failures of plastic components in service, was first documented approximately 75 years ago for wire and cable jacketing made by the Western Electric Company from low density polyethylene (LDPE) which was experiencing stress-induced failure [29, 31-33]. Investigations by Bell Laboratories, a research division of Western Electric, traced the failure of the PE cable sheathing to a soap used to ease the drawing of wires through conduits. This environmental cracking led to the subsequent creation of a standardized test, known as the Bell Test (ASTM D1693), that is still used today to evaluate a polymer’s environmental stress cracking resistance (ESCR) [31, 34].

To adequately comprehend the failure mechanism of ESC, some background knowledge on corresponding cracking in an inert medium, such as air or water, is necessary. Cracking in the absence of an active medium (like an ESC agent) occurs while enduring prolonged static stresses, in a mechanism known as slow crack growth (SCG). SCG is a multi-step brittle fracture mode that develops over time as a result of molecular disentanglement among the polymer chains due to the continuous application of stress. The process of SCG starts with craze initiation, followed by craze growth which leads to crack initiation, then crack extension, and finally catastrophic fracture. The crazing phenomenon entails a network of cross-tied fibrils across the craze planes (which are perpendicular to the main stretch direction) from which the network grows by pulling out fresh material from a "stress activated active zone". These crazes as a phenomenon are first created when they propagate and are terminated by turning into a crack [35]. They initiate when an external stretch causes development of a microscopic void at a stress concentrated region created by a pre-existing defect such as a notch. The void then propagates perpendicular to the highest principal stress while maintaining stability through the fibrils spanning the craze. The fibrils will eventually fail, resulting in a craze-crack transition and subsequently complete failure [36, 37].

In order to attain a better understanding of SCG in PE, it is important to understand the molecular topology of a semi-crystalline polymer. The mechanical properties of semi-crystalline polymers are believed to be governed primarily by the presence of intra-crystalline molecular connections, such as tie molecules (TMs) (chains that begin and end in adjacent crystalline lamella), cilia (chain ends protruding from crystallites), and loose loops (chains that begin and end in the same lamella). These connections traversing through the amorphous regions hold crystallites in proximity to one another together, preventing them from slipping or splitting under stresses which would otherwise result in macroscopic brittleness of the material [38, 39]. TMs have been recognized as being the most important of possible crystalline/amorphous interactions for their influence on short-term properties, such as stiffness and strength, as well as the long-term properties of semi-crystalline polymers [38]. They are high molecular weight polymer chains that span the amorphous region connecting the crystal lamella together.

Loose loops or cilia in the amorphous regions entangle to give rise to a weaker interaction that helps hold the crystalline structure together [38]. The application of a load normal to the face of a crystalline lamellae causes the TMs to stretch; and after some time the long-term low-level stress causes the TMs to extend and ultimately fail until their numbers are insufficient to withstand the load applied; slippage or breakage of adjacent lamella occurs, which generates a void; and consequently, crazing begins which ultimately leads to the SCG behaviour mentioned above [39].

The mechanism behind ESC can mostly be described by SCG, with its main difference being the accelerated failure due to the presence of an active medium. The environment/surrounding medium in contact with polymer is believed to be absorbed into the polymer despite its general incompatibility, resulting in subsequent lubrication of the intra-crystalline molecular connections and consequently premature material failure under SCG conditions. Various authors believe that this absorption must be localized to the amorphous phase [40-43], while others like Ward et al. [44] have proposed that the active medium could also diffuse inside the crystals. Alcohols, fatty acid methyl esters (FAME), animal fats, vegetable oils, and mineral oils are all possible examples of ESC agents identified through the use of the Bell Test; an excellent example for an active agent is Igepal CO630 (Nonylphenoxy poly(ethyleneoxy) ethanol), so much so that it has become the standardized environment to execute the Bell Test as well as many other ESCR testing procedures, due to its ability of effectively accelerating failure in environmentally stable polymers [31].

Several methodologies have been proposed to explain the precise molecular mechanism leading to ESC but to this day the mode of failure remains a matter of debate [40-43, 45, 46]. For over a decade, two theories that attempt to explain ESC have existed primarily in one form or the other [46]. An initial explanation of the mechanism of ESC noted that exposure to an active medium causes a reduction in the surface energy for crack formation which allows for lower stresses to cause craze or crack formation in comparison to inert environments [37, 46, 47]. In other words, the required stress for crack formation is lowered when the material is exposed to an active medium, since the solid/liquid interfacial tension is lower than solid/air interface allowing for crack formation. The following hypothesis may be an asset to the ESC mechanism, but it is believed to be a minor aspect when considering the overall mechanism [29]. In the second theory, the medium generates more internal changes by acting as a plasticizer [46]. In other words, limited plasticization by the medium reduces the glass transition temperature ($T_g$) of the polymer to a degree where the application of a necessary amount of stress causes the glass to flow like a liquid in the direction of stress [29, 46]. Rogers et al. [48] proposed an excellent mechanism for ESC of PE which has been used in the coming chapters to provide an explanation of the mechanism for biodiesel acting as an ESC agent to PE. Rogers et al. recognized that Igepal CO630, which is a commercial detergent, contains small amounts of impurities (approximately 1%), such a nonylphenol and PE glycol, and those species may be the cause of cracking for PE. Since nonylphenol is not soluble in water but is soluble in the detergent, it is carried within a micelle in water to the PE surface. The solubility parameter (total cohesive attraction between the fluid molecules) of nonylphenol (19.3 $\mathrm{MPa}^{\frac{1}{2}}$ ) is close to that of PE (16.4 $\mathrm{MPa}^{\frac{1}{2}}$) [49]. As a result, a concentration-limited plasticization mechanism seems to be responsible for crack propagation. The following is the commonly proposed crack propagation mechanism for ESC of PE in the Bell Test [48]:

1. Fibrillated fractures occur at the crack tip of the bent specimens.
2. The fluid media contacts the fibrillated surface inside the crack and preferentially diffuses to areas where the stresses are highest. Absorption of the contaminant bound in micelles will plasticize the polymer to reduce the strength of its tie chains in the amorphous regions of fibrils.
3. Stress-enhanced diffusion takes place at the ends (shoulders) of the fibrils. The shoulders have the most disrupted morphological structure as a result, which helps diffusion and sorption.
4. The concentrated stresses in the crack tip region cause the plasticized tie chains to fail and the crack grows as a result.

This model of the process is useful in understanding gross features of the phenomenon.

Modern research into ESC has focused on finding polymeric properties and environmental conditions that would improve overall ESCR of the polymer. Early research has recurrently suggested ESC can occur in mobile polar liquids [50], but it is not clear if this applies to all stress cracking materials [49]. Hittmair and Ullman [51] studied the effects of Igepal concentration and temperature on ESC, showing that the solubility of the liquid in the polymer increased with increasing stress. Lustiger et al. [52]

proposed a basic mechanism of ESC based on the ability of Igepal to diffuse in between the more highly deformed crystalline regions inside the specimens, causing “stress-induced plasticization” and promoting slip between adjacent lamellae. The aggressiveness of Igepal was traced back to its ability to diffuse into the amorphous (interlamellar) region of the polymer. The peak aggressiveness of Igepal has been found to be at approximately 50%, with lower activity found at the maximum (100%) and minimum (0%) concentrations [51, 53-55]. However, 10% and 100% Igepal solutions are most commonly used in ESCR tests.

Early researchers suggested that the fluid’s total solubility parameter was the most important factor affecting the ESCR of the polymer. If the solubility parameter between the fluid molecules is equal to or close to that of the polymer molecules, then the particular fluid/polymer pair would be miscible, making the plastic susceptible to ESC [30]. Brown [49] showed the aggressiveness of Igepal by depicting the similarity of the solubility parameter of Igepal CO630 (20 $MPa^{\frac{1}{2}}$) to that of PE (16.4 $MPa^{\frac{1}{2}}$). ESCR studies [56] have also reported that fluids of very low molecular weight in PE have a negative impact on the mechanical properties of PE, resulting in embrittlement. Fluids are usually more aggressive at temperatures near their boiling points. For example, nitrogen is a stress cracking agent for several plastics at its boiling point (-196 ℃) [30]. Since fluids with a high molar volume tend to have high tend to have high viscosities and high boiling points, they are less likely to be severe stress cracking agents [30].

Carey [57] studied the stress and temperature dependency of the failure times of PE samples using a test based on conveying a constant uniaxial tension to the sample. Results showed that time to failure decrease with increasing temperature. Using a similar test method, Lander and Carey [58] investigated the effects of density and melt index on failure time for branched and linear PEs. Investigations predicted that PE samples with higher crystallinity/density and higher molecular weight (lower Melt flow index (MFI)) showed more resistance to ESC when compared on the basis of equivalent stress [8, 30, 58]. The closely packed crystals in the high density materials resist ESC by acting as a barrier to fluid penetration and evidently stopping the cracking from occurring, meaning that thermoplastics with more amorphous content will be more susceptible to ESC [30, 51, 59]. It is important to note there is an ambiguity in finding a potential correlation between the resistance of a polymer to ESC and its crystallinity, which can be attributed to other properties of the polymer that also affect ESCR [60]. Apart from molecular weight and crystallinity, chain branching has also been found to increase resistance to ESC. Huang and Brown [61] were able to show a decrease in the rate of SCG with increasing branches. This phenomenon is attributed to the idea that chain branching decreases the average thickness of the lamellar which increases the overall probable formation of TMs, resulting in a more resistant polymer to ESC. Building on this, Yeh at al. [62] were able to show that the presence of short chain branches slowed the diffusion of Igepal into the polymer, increasing their failure time.

A theoretically crucial factor in ESC is the localized fluid absorption. The absorption of any fluid plasticizes the polymer causing loss in yield strength; and the greater the concentration of the fluid absorbed, the lower the yield strength of the polymer [49]. Presence of a pre-existing defect, such as a notch, in the polymeric material results in the creation of a localized stress field in front of the defect. Studies by Hittmair and Ullman [51] show increasing solubility of the liquid in the polymer with increasing stresses. Thus, adsorption of the fluid into the material occurs preferentially at the fibrils of the localized stress field where stresses are highest and surface area is greatest for the PE immersed within the fluid [48]. The absorbed fluid plasticizes the polymer at the high stress region reducing the strength of the tie chains in the amorphous regions of the crystals. The diffusion constant of the absorbed fluid drops in highly oriented regions of the fibrils; however the thermodynamics of the system demands the polymer finding a lower energy state. Hence, stress-enhanced diffusion is expected to take place at the ends (shoulders) of the fibrils causing the zone to progressively grow perpendicularly to the applied stress, and evidently leading to crazing and cracking [30, 48]. Conversely, an environment that has great affinity to the polymer will cause whole body absorption to occur very rapidly, swamping local absorption and causing the surface to soften without cracking [30].

## 2.3. The Bell Test and other test methods for environmental stress cracking resistance

Numerous quick laboratory-scale test methods for ESCR have been established to serve as rapid real-life predictions of ESC behavior. The industrial purpose behind these accelerated ESC conditions is to attain a quick rank of different materials as a function of their ESCR for part design & quality control, evaluation of competitive products, and research & development [41]. The test methods developed can be divided into two groups, those deforming at constant strain and deforming at constant stress. The first group is considered less severe than tests at constant stress, since stresses are allowed to relax in the former case.

The low cost and simplicity of constant strain methods have made them the more popular testing methods. The Bell Test (ASTM D1693) is one of the most commonly used test methods for quantifying the ESCR of PE [31, 34]. It involves the immersion of a brass channel holding ten (10) bent and notched samples of PE (38 x 13 x 3 mm), into a test tube filled with an ESC agent, preferably Igepal CO630, at elevated temperatures [34]. The test is run at conditions that promote shorter test times by speeding up failure with either a 100% or 10% concentration of the stress cracking agent at 50 ℃ (Condition A and B) or 100% at 100 ℃ (Condition C) [34]. The ESCR value ($F_{50}$ hours) is then stated as the number of hours it takes to visually detect failure of 50% of the samples. Despite the simplicity and popularity of the Bell Test, several limitations including poor accuracy (due to visual inspection being the only failure detection method) and long testing times have limited the benefits of this test.

The notched constant tensile load test (NCTL) (ASTM D5397) [63] was developed as an improvement to the Bell Test for geomembranes. It involves immersion of a notched dog-bone (dumbbell) shaped sample into a 10% Igepal solution at 50 ℃. The sample is loaded with progressively increasing stresses ranging from 20-65% at max increments of 5%; and the time of failure is recorded. The NCTL serves as an improvement to the Bell Test by removing the possibility of stress relaxation; but due to the ability of evaluating only one sample at a time, testing takes a longer time overall in comparison to the Bell Test.

The Pennsylvania Notch Test (PENT) (ASTM F1473) [64] was developed as another constant stress test method for resistance to SCG but with the focus on PE pipes. Notched rectangular shaped samples under constant stress (2.4 MPa) at 80 ℃ are observed for the progression of SCG; and time to failure is recorded. Unlike the previous tests, three coplanar notches are used to increase stress concentration on the sample. The following test focuses on measuring the SCG resistance of the samples, which is the proposed mechanism behind ESC.

The test methods available for ESCR have been known to produce dissimilar results that contradict each other and fail to predict, with reasonable accuracy, polymer performances in industrial applications. This lack of accuracy and robustness has prompted the need to develop new test methods and improve already existing ones.

## 2.4. Nonlinear ultrasonic testing

For many years the characterization of semi-crystalline polymers has been a challenge in the polymer manufacturing industry, especially to see structural aspects below their yielding point. The shortage of accurate nondestructive testing methods for the evaluation of solvent swelling and ESC in plastics has made research into adopting new tools and procedures for characterization of semi-crystalline polymers a matter of importance. The few existing nondestructive characterization techniques that evaluate solvent penetration are mostly focused on spectroscopic analysis that rely upon the propagation of electromagnetic or mechanical waves, such as infrared, UV-VIS, X-ray, acoustic, and ultrasonic testing. Despite the potential of spectroscopic analysis, limitations on their performance in the polymer industry are brought about by the heterogenous morphology of the plastic products (that are usually thermal and acoustic insulators) and their strong dependency on preparation conditions. Another limiting aspect of polymer characterization is the selection between local characterization, which may not be an effective representation of the whole, or bulk characterization, which is limited due to existing physical constraints. For example, infrared spectroscopy has been used to track the penetration of chemical constituents of solvent molecules through thin films and at the surface of thicker materials [65, 66]. Despite this technique being effective in providing an analysis that is constrained to a small and localized region, it is limited by its inability to imply what is happening to the bulk of the polymer.

The observation of spectroscopic variations through nonlinear ultrasonic testing, for evaluation of the penetration of small molecules into PE and giving bulk assessments of the internal stresses and microstructural modifications to the semi-crystalline morphology of the plastic, has been shown to be a promising technique [67]. It is one of the only test methods known to assess internal stresses in semi-crystalline materials for elastic deformations. The following characterization technique is based on the interaction of mechanical waves with the material. Traditional acoustic measurements use a pulse-echo test to calculate the ultrasonic velocity and signal attenuation per unit propagation distance for analyzing polymeric materials; but these effects are based on pure elastic propagation of the planar waves through a solid material and unlike metals and ceramics that propagate mechanical waves better, polymers cause a higher attenuation of the waves [68-70]. Higher signal attenuation is seen with increasing crystallinity [71]. The use of this technique with polymeric materials requires amplification of received signals and good coupling of the transducer with the sample.

An alternate test to the pulse-echo method is to use guided wave propagation that relies on the principle of planar or plate waves. The high attenuation of the ultrasonic waves caused by the viscoelastic nature of the semi-crystalline polymers makes the guided wave test advantageous over the pulse-echo test, allowing for investigation of larger areas [72]. In this test, two sensors are placed on different spots along the surface of the sample; the first emits the ultrasonic waves and the second receives the waves after propagation through the polymeric material. The propagation of these waves over long distances in the sample is amplified by their reflection off of geometric boundaries, but this amplification is dependant on the frequency of the waves [73]. The nonlinear propagation of the ultrasonic waves is affected by the significantly different elastic properties of the internal structure of the polymer as well as internal defects causing a mismatch of stress transmitter elements [74].

The propagation of ultrasonic waves through a microstructure with discontinuities, similar to those created by the penetration of a solvent in the semi-crystalline network, generates frequencies different from original wave introduced [15, 67]. The observed harmonics have been shown to be directly related to the occurrence of nonlinearities in the structure of the material [75]. Higher internal stresses and defects in the material have been shown to generate higher harmonic peaks in several materials, including semi-crystalline polymers [15, 67, 76].

## References

[1] A.C. Pinto, L.L.N. Guarieiro, M.J.C. Rezende, N.M. Ribeiro, E.A. Torres, W.A. Lopes, et al., Biodiesel: an overview, Journal of the Brazilian Chemical Society. 16 (2005) 1313–1330. doi:10.1590/s0103-50532005000800003.

[2] E. Shay, Diesel fuel from vegetable oils: Status and opportunities, Biomass and Bioenergy. 4 (1993) 227–242. doi:10.1016/0961-9534(93)90080-n.

[3] G. Knothe, Krahl JÃ¼rgen, J.V. Gerpen, The Biodiesel Handbook, Elsevier Science, 2015.

[4] J.V. Gerpen, Biodiesel processing and production, Fuel Processing Technology. 86 (2005) 1097–1107. doi:10.1016/j.fuproc.2004.11.005.

[5] E. Richaud, Flaconnèche Bruno, J. Verdu, Biodiesel permeability in polyethylene, Polymer Testing. 31 (2012) 170–1076. doi:10.1063/1.4738433.

[6] M. Böhning, U. Niebergall, A. Adam, W. Stark, Influence of biodiesel sorption on temperature-dependent impact properties of polyethylene, Polymer Testing. 40 (2014) 133–142. doi:10.1016/j.polymertesting.2014.09.001.

[7] M. Schilling, M. Böhning, H. Oehler, I. Alig, U. Niebergall, Environmental stress cracking of polyethylene high density (PE-HD) induced by liquid media - Validation and verification of the full-notch creep test (FNCT), Materialwissenschaft Und Werkstofftechnik. 48 (2017) 846–854. doi:10.1002/mawe.201700065.

[8] M.M. Maru, M.M. Lucchese, C. Legnani, W.G. Quirino, A. Balbo, I.B. Aranha, et al., Biodiesel compatibility with carbon steel and HDPE parts, Fuel Processing Technology. 90 (2009) 1175–1182. doi:10.1016/j.fuproc.2009.05.014.

[9] M. Böhning, U. Niebergall, A. Adam, W. Stark, Impact of biodiesel sorption on mechanical properties of polyethylene, Polymer Testing. 34 (2013) 17–24. doi:10.1016/j.polymertesting.2013.12.003.

[10] M. Böhning, U. Niebergall, M. Zanotto, V. Wachtendorf, Impact of biodiesel sorption on tensile properties of PE-HD for container applications, Polymer Testing. 50 (2016) 315–324. doi:10.1016/j.polymertesting.2016.01.025.

[11] M. Weltschev, J. Werner, M. Haufe, M. Heyer, Compatibility of High-Density Polyethylene Grades with Biofuels, Packaging Technology and Science. 27 (2013) 231–240. doi:10.1002/pts.2028.

[12] M. Thompson, B. Mu, C. Ewaschuk, Y. Cai, K. Oxby, J. Vlachopoulos, Long term storage of biodiesel/petrol diesel blends in polyethylene fuel tanks, Fuel. 108 (2013) 771–779. doi:10.1016/j.fuel.2013.02.040.

[13] W. Trakarnpruk, S. Porntangjitlikit, Palm oil biodiesel synthesized with potassium loaded calcined hydrotalcite and effect of biodiesel blend on elastomer properties, Renewable Energy. 33 (2008) 1558–1563. doi:10.1016/j.renene.2007.08.003.

[14] B. Flitney, Which elastomer seal materials are suitable for use in biofuels?, Sealing Technology. 2007 (2007) 8–11. doi:10.1016/s1350-4789(07)70409-9.

[15] A. Saad, F. Gomes, M. Thompson, Plasticizing effect of oxidized biodiesel on polyethylene observed by nondestructive method, Fuel. 252 (2019) 246–253. doi:10.1016/j.fuel.2019.04.122.

[16] G. Lutz, J.F. Mata-Segreda, Kinetics of interaction of palm ethyl biodiesel with three different polymer materials, Journal of Physical Organic Chemistry. 21 (2008) 1068–1071. doi:10.1002/poc.1427.

[17] H.J. Nieschlag, I.A. Wolff, Industrial uses of high erucic oils, Journal of the American Oil Chemists Society. 48 (1971) 723–727. doi:10.1007/BF02638529.

[18] P.P. Kundu, Improvement of filler-rubber interaction by the coupling action of vegetable oil in carbon black reinforced rubber, Journal of Applied Polymer Science. 75 (1999) 735–739. doi:10.1002/(sici)1097-4628(20000207)75:6<735::aid-app1>3.0.co;2-t.

[19] V. Nandanan, R. Joseph, K.E. George, Rubber seed oil: A multipurpose additive in NR and SBR compounds, Journal of Applied Polymer Science. 72 (1999) 487–492. doi:10.1002/(sici)1097-4628(19990425)72:4<487::aid-app4>3.0.co;2-m.

[20] J. Wehlmann, Use of esterified rapeseed oil as plasticizer in plastics processing, Lipid - Fett. 101 (1999) 249–256. doi:10.1002/(sici)1521-4133(199907)101:7<249::aid-lipi249>3.0.co;2-i.

[21] F. Cataldo, O. Ursini, G. Angelini, Biodiesel as a Plasticizer of a SBR-Based Tire Tread Formulation, ISRN Polymer Science. 2013 (2013) 1–9. doi:10.1155/2013/340426.

[22] J.-M. Restrepo-Flórez, A. Bassi, M.R. Thompson, Microbial degradation and deterioration of polyethylene – A review, International Biodeterioration & Biodegradation. 88 (2014) 83–90. doi:10.1016/j.ibiod.2013.12.014.

[23] R. Mccormick, M. Ratcliff, L. Moens, R. Lawrence, Several factors affecting the stability of biodiesel in standard accelerated tests, Fuel Processing Technology. 88 (2007) 651–657. doi:10.1016/j.fuproc.2007.01.006.

[24] M. Fazal, A. Haseeb, H. Masjuki, Biodiesel feasibility study: An evaluation of material compatibility; performance; emission and engine durability, Renewable and Sustainable Energy Reviews. 15 (2011) 1314–1324. doi:10.1016/j.rser.2010.10.004.

[25] J. Pullen, K. Saeed, An overview of biodiesel oxidation stability, Renewable and Sustainable Energy Reviews. 16 (2012) 5924–5950. doi:10.1016/j.rser.2012.06.024. J. Pullen, K. Saeed, An overview of biodiesel oxidation stability, Renewable and Sustainable Energy Reviews. 16 (2012) 5924–5950. doi:10.1016/j.rser.2012.06.024.

[26] S. Jain, M. Sharma, Stability of biodiesel and its blends: A review, Renewable and Sustainable Energy Reviews. 14 (2010) 667–678. doi:10.1016/j.rser.2009.10.011.

[27] E. Richaud, B. Fayolle, J. Verdu, J. Rychlý, Co-oxidation kinetic model for the thermal oxidation of polyethylene-unsaturated substrate systems, Polymer Degradation and Stability. 98 (2013) 1081–1088. doi:10.1016/j.polymdegradstab.2013.01.008.

[28] E. Richaud, F. Djouani, B. Fayolle, J. Verdu, B. Flaconneche, New Insights in Polymer-Biofuels Interaction, Oil & Gas Science and Technology – Revue d'IFP Energies Nouvelles. 70 (2013) 317–333. doi:10.2516/ogst/2013151.

[29] L.M. Robeson, Environmental stress cracking: A review, Polymer Engineering & Science. 53 (2012) 453–467. doi:10.1002/pen.23284.

[30] D. Wright, Environmental stress cracking of plastics, Rapra, Shawbury, 1996.

[31] J.B. Decoste, F.S. Malm, V.T. Wallder, Cracking of Stressed Polyethylene, Industrial & Engineering Chemistry. 43 (1951) 117–121. doi:10.1021/ie50493a035.

[32] J. Jansen, Plastic Failure through Environmental Stress Cracking, Plastics Engineering. 71 (2015) 30–36. doi:10.1002/j.1941-9635.2015.tb01435.x.

[33] J.C. Arnold, Environmental stress crack initiation in glassy polymers, Trends in Polymer Science. 4 (1996) 403–408.

[34] ASTM International. ASTM D1693-15 Standard Test Method for Environmental Stress-Cracking of Ethylene Plastics. West Conshohocken, PA: ASTM International, 2015. Web. 31 Mar 2017.

[35] R.A. Deblieck, D.V. Beek, K. Remerie, I.M. Ward, Failure mechanisms in polyolefines: The role of crazing, shear yielding and the entanglement network, Polymer. 52 (2011) 2979–2990. doi:10.1016/j.polymer.2011.03.055.

[36] E.J. Kramer, Microscopic and molecular fundamentals of crazing, Crazing in Polymers Advances in Polymer Science. (1983) 1–56. doi:10.1007/bfb0024055.

[37] H.R. Brown, A molecular interpretation of the toughness of glassy polymers, Macromolecules. 24 (1991) 2752–2756. doi:10.1021/ma00010a018.

[38] R. Seguela, Critical review of the molecular topology of semicrystalline polymers: The origin and assessment of intercrystalline tie molecules and chain entanglements, Journal of Polymer Science Part B: Polymer Physics. 43 (2005) 1729–1748. doi:10.1002/polb.20414.

[39] A. Lustiger, R. Markham, Importance of tie molecules in preventing polyethylene fracture under long-term loading conditions, Polymer. 24 (1983) 1647–1654. doi:10.1016/0032-3861(83)90187-8.

[40] M. Chan, J. Williams, Slow stable crack growth in high density polyethylenes, Polymer. 24 (1983) 234–244. doi:10.1016/0032-3861(83)90139-8.

[41] J.M. Lagarón, J.M. Pastor, B.J. Kip, Role of an active environment of use in an environmental stress crack resistance (ESCR) test in stretched polyethylene: Polymer. 40 (1999) 1629–1636. doi:10.1016/s0032-3861(98)00406-6.

[42] A. Lustiger, R.D. Corneliusen, The effect of an environmental stress cracking agent on interlamellar links in polyethylene, Journal of Polymer Science Part B: Polymer Physics. 24 (1986) 1625–1629. doi:10.1002/polb.1986.090240719.

[43] X. Lu, R. Qian, N. Brown, The effect of crystallinity on fracture and yielding of polyethylenes, Polymer. 36 (1995) 4239–4244. doi:10.1016/0032-3861(95)92219-5.

[44] A. Ward, X. Lu, Y. Huang, N. Brown, The mechanism of slow crack growth in polyethylene by an environmental stress cracking agent, Polymer. 32 (1991) 2172–2178. doi:10.1016/0032-3861(91)90043-i.

[45] A.N. Gent, Hypothetical mechanism of crazing in glassy plastics, Journal of Materials Science. 5 (1970) 925–932. doi:10.1007/bf00558171.

[46] G.A. Bernier, R.P. Kambour, The Role of Organic Agents in the Stress Crazing and Cracking of Poly(2,6-dimethyl-1,4-phenylene oixde), Macromolecules. 1 (1968) 393–400. doi:10.1021/ma60005a005.

[47] L.E. Nielsen, The apparent domain structure of polystyrene as revealed by liquid and vapor crazing, Journal of Applied Polymer Science. 1 (1959) 24–27. doi:10.1002/app.1959.070010105.

[48] C.E. Rogers, Stress Cracking of Polyethylene in Organic Liquids., (1986). doi:10.21236/ada165733.

[49] H. Brown, A theory of the environmental stress cracking of polyethylene, Polymer. 19 (1978) 1186–1188. doi:10.1016/0032-3861(78)90069-1.

[50] J.B. Howard, Why do plastics stress-crack?, Polymer Engineering and Science. 5 (1965) 125–129. doi:10.1002/pen.760050307.

[51] P. Hittmair, R. Ullman, Environmental stress cracking of polyethylene, Journal of Applied Polymer Science. 6 (1962) 1–14. doi:10.1002/app.1962.070061901.

[52] A. Lustiger, R.D. Corneliussen, Environmental stress crack growth in high-density polyethylene, Journal of Polymer Science: Polymer Letters Edition. 17 (1979) 269–275. doi:10.1002/pol.1979.130170504.

[53] R. Qian, X. Lu, N. Brown, The effect of concentration of an environmental stress cracking agent on slow crack growth in polyethylenes, Polymer. 34 (1993) 4727–4731. doi:10.1016/0032-3861(93)90708-i.

[54] M. Rink, R. Frassine, P. Mariani, G. Carianni, Effects of Detergent on Crack Initiation and Propagation in Polyethylenes, European Structural Integrity Society. (2003) 103–114. doi:10.1016/s1566-1369(03)80087-0.

[55] R. Ayyer, A. Hiltner, E. Baer, Effect of an environmental stress cracking agent on the mechanism of fatigue and creep in polyethylene, Journal of Materials Science. 43 (2008) 6238–6253. doi:10.1007/s10853-008-2926-1.

[56] I.L. Hopkins, W.O. Baker, J.B. Howard, Complex Stressing of Polyethylene, Journal of Applied Physics. 21 (1950) 206–213. doi:10.1063/1.1699636.

[57] R.H. Carey, Creep and Stress-Rupture Behavior of Polyethylene Resins, Industrial & Engineering Chemistry. 50 (1958) 1045–1048. doi:10.1021/ie50583a040.

[58] L.L. Lander, R.H. Carey, Polyethylene—Environmental Stress Rupture and Blown Bottles, Symposium on Simulated Service Testing of Packaging. (n.d.). doi:10.1520/stp47053s.

[59] S. Bandyopadhyay, H.R. Brown, Evidence of interlamellar failure in environmental stress cracking of polyethylene, Journal of Materials Science. 12 (1977) 2131–2134. doi:10.1007/bf00561990.

[60] P. Sardashti, A.J. Scott, C. Tzoganakis, M.A. Polak, A. Penlidis, Effect of Temperature on Environmental Stress Cracking Resistance and Crystal Structure of Polyethylene, Journal of Macromolecular Science, Part A. 51 (2014) 189–202. doi:10.1080/10601325.2014.871934.

[61] Y.-L. Huang, N. Brown, The dependence of butyl branch density on slow crack growth in polyethylene: Kinetics, Journal of Polymer Science Part B: Polymer Physics. 28 (1990) 2007–2021. doi:10.1002/polb.1990.090281110.

[62] J.T. Yeh, J.-H. Chen, H.-S. Hong, Environmental stress cracking behavior of short-chain branch polyethylenes in Igepal solution under a constant load, Journal of Applied Polymer Science. 54 (1994) 2171–2186. doi:10.1002/app.1994.070541320.

[63] ASTM D 5397 – Standard Test Method for Evaluation of Stress Crack Resistance of Polyolefin Geomembranes Using Notched Constant Tensile Load Test, 2007.

[64] ASTM International. ASTM F1473-16 Standard Test Method for Notch Tensile Test to Measure the Resistance to Slow Crack Growth of Polyethylene Pipes and Resins. West Conshohocken, PA: ASTM International, 2016. Web. 31 Mar 2017.

[65] D. Cava, R. Catala, R. Gavara, J.M. Lagaron, Testing limonene diffusion through food contact polyethylene by FT-IR spectroscopy: Film thickness, permeant

concentration and outer medium effects, Polymer Testing. 24 (2005) 483–489. doi:10.1016/j.polymertesting.2004.12.003.

[66] M. Wang, P. Wu, S.S. Sengupta, B.I. Chadhary, J.M. Cogen, B. Li, Investigation of Water Diffusion in Low-Density Polyethylene by Attenuated Total Reflectance Fourier Transform Infrared Spectroscopy and Two-Dimensional Correlation Analysis, Industrial & Engineering Chemistry Research. 50 (2011) 6447–6454. doi:10.1021/ie102221a.

[67] F. Gomes, W. West, M. Thompson, Effects of annealing and swelling to initial plastic deformation of polyethylene probed by nonlinear ultrasonic guided waves, Polymer. 131 (2017) 160–168. doi:10.1016/j.polymer.2017.10.041.

[68] V.K. Kinra, V.R. Iyer, Ultrasonic measurement of the thickness, phase velocity, density or attenuation of a thin-viscoelastic plate. Part II: the inverse problem, Ultrasonics. 33 (1995) 111–122. doi:10.1016/0041-624x(94)00026-l.

[69] B. Zhao, O. Basir, G. Mittal, Estimation of ultrasound attenuation and dispersion using short time Fourier transform, Ultrasonics. 43 (2005) 375–381. doi:10.1016/j.ultras.2004.08.001.

[70] A. Bernard, M.J.S. Lowe, M. Deschamps, Guided waves energy velocity in absorbing and non-absorbing plates, The Journal of the Acoustical Society of America. 110 (2001) 186–196. doi:10.1121/1.1375845.

[71] K. Adachi, G. Harrison, J. Lamb, A.M. North, R.A. Pethrick, High frequency ultrasonic studies of polyethylene, Polymer. 22 (1981) 1032–1039. doi:10.1016/0032-3861(81)90287-1.

[72] B. Hosten, M. Castaings, Comments on the ultrasonic estimation of the viscoelastic properties of anisotropic materials, Composites Part A: Applied Science and Manufacturing. 39 (2008) 1054–1058. doi:10.1016/j.compositesa.2008.02.013.

[73] M. Mitra, S. Gopalakrishnan, Guided wave based structural health monitoring: A review, Smart Materials and Structures. 25 (2016) 053001. doi:10.1088/0964-1726/25/5/053001.

[74] K.-Y. Jhang, Nonlinear ultrasonic techniques for nondestructive assessment of micro damage in material: A review, International Journal of Precision Engineering and Manufacturing. 10 (2009) 123–135. doi:10.1007/s12541-009-0019-y.

[75] C.J. Lissenden, Y. Liu, J.L. Rose, Use of non-linear ultrasonic guided waves for early damage detection, Insight - Non-Destructive Testing and Condition Monitoring. 57 (2015) 206–211. doi:10.1784/insi.2015.57.4.206.

[76] V.K. Chillara, C.J. Lissenden, Review of nonlinear ultrasonic guided wave nondestructive evaluation: theory, numerics, and experiments, Optical Engineering. 55 (2015) 011002. doi:10.1117/1.oe.55.1.011002.

# Chapter

# 3. Plasticizing Effect of Oxidized Biodiesel on Polyethylene Observed by Nondestructive Method

# Plasticizing effect of oxidized biodiesel on polyethylene observed by nondestructive method

A.K. Saad, F.P.C. Gomes, M.R. Thompson*

Department of Chemical Engineering, CAPPA-D/MMRI

McMaster University, Hamilton, Ontario, Canada

Published manuscript at Fuel ©Elsevier

DOI: 10.1016/j.fuel.2019.04.122

**Author contribution:**

The first author, A.K. Saad, was responsible for the design of experiments, execution of gravimetric analysis, and other characterization techniques. The author was also responsible for writing majority of the manuscript as well as submission and publishing of manuscript. The second author, F.P.C. Gomes, contributed to the study by supervising and aiding in the design of experiments, as well as execution of ultrasonic and mechanical testing of the samples, and writing of parts of the manuscript and revision of it. The author, M.R. Thompson, was responsible for supervision of the design and completion of experiments as well as revision of the manuscript.

**Main scientific contributions of the paper:**

- Use of a novel nondestructive testing method based on ultrasonics to investigate the effects of biodiesel as a plasticizer for polyethylene.
- Demonstration of the different modes of plasticization by biodiesel and toluene.
- Analysis of the effect of degradation on the plasticizing capability of biodiesel.

## Abstract

This paper explores the compatibility of biodiesel with different grades of polyethylene, specifically examining the extent of plasticization in order to gain a better understanding of the biofuel’s compatibility with this common polymer. Its bulk influences on polyethylene were investigated by gravimetric and mechanical testing, and by the application of a newly developed nondestructive ultrasonic testing method. Diffusion rates and the extent of plasticization by biodiesel were compared to results obtained with toluene, a known plasticizer for polyethylene. Mechanical and gravimetric analysis showed that biodiesel exhibited bulk attributes of a plasticizer for the tested polyethylenes with reduced moduli proportional to the amount of fuel uptake and that uptake was inversely proportional to crystalline content of the polymer. Based on uptake amounts, the efficiency of biodiesel as a plasticizer towards polyethylene was found to be more than double that of toluene. However, spectral analysis by ultrasonics showed that absorbed toluene and biodiesel influenced the microstructure of polyethylene differently. Notable differences in internal stresses were noted between the two fluids for the same amount absorbed. A subsequent study analyzed the impact that biodiesel degradation had on plasticization. Although the trend showed a slight change in diffusion rate with increasing oxidation of the medium, the mechanical and ultrasonic results did not show significant differences between fresh and degraded biodiesel within the 45 days span of the test. Combining the evidence observed in this study, a mechanism is proposed for biodiesel plasticization that can help with failure prevention and material selection.

**Keywords:** Compatibility; Ultrasonic Testing; Ageing; Toluene.

## 3.1. Introduction

The use of polymers in parts design that will be exposed to chemicals always generates routine compatibility concerns. Thus, designers require proper identification of any chemical and physical interactions that would undermine the functionality of a manufactured part. Polyethylene (PE) is a common material used for chemicals storage including fuel tanks in automobiles, marine vessels and agricultural machinery [1]. Recently, biodiesel has emerged as a viable bio-sourced fuel alternative to fossil fuels, presently blended at low fractions with diesel, making it a relevant compatibility concern for polyethylene fuel tanks. Most of the biodiesel compatibility studies on polymers other than polyethylene have focused on elastomers, which reported swelling with a corresponding decline in mechanical properties [2,3]. A few recent studies on polyethylene [4-11] have suggested interactions with biodiesel may be quite aggressive.

A small number of long-term compatibility studies with biodiesel have reported swelling with notable weight gains and discoloration of high density polyethylene (HDPE) [4,7-9,11]. Several of these studies [8,9,11] reported on the plasticizing nature of biodiesel, shown by a marked decrease of Young's Modulus and increase of the stain-at-max stress, which was related to the concentration of absorbed fuel in the polymer. Relevant factors affecting absorption of biodiesel into polyethylene, such as the polymer crystalline morphology and changes in biodiesel chemistry due to degradation have not yet been studied. However, related studies have shown fatty acids and vegetable oils to be effective plasticizers in different polymers and rubbers [12-17].

An often overlooked shortcoming of biodiesel in compatibility testing is its changing chemical and physical properties associated with oxidation. Biodiesel is susceptible to degradation and does so more rapidly with heating, generating several by-products including free fatty acids [11,18-20]. Some studies [7,11] have found no effect of biodiesel degradation on polyethylene, chemically, over more than a year of observation while others [9,10,21,22] reported accelerated oxidative degradation of polyethylene by the formed unsaturated fatty acids during aging. The differences may be attributed to the different testing environments in these studies. Whether those degradation products of biodiesel exhibit differing absorption and plasticization effects on polyethylene has yet to be considered.

External plasticization of polyethylene is commonly correlated with the diffusion of penetrants over a certain exposure time that can be monitored either gravimetrically or by analysis of mechanical properties [23]. The latter is more definitive, since mass changes may be difficult to detect, though it is considered a destructive characterization method and that is often undesirable. Nuclear magnetic resonance (NMR) has been applied to evaluate the penetration of solvents into different morphologies of polyethylene, showing diffusion on the amorphous phase, but this approach would also fall under the destructive category of evaluations [24]. Few nondestructive characterization techniques exist for this characterization; most of them are focused on spectroscopic analysis. Infrared spectroscopy can track the penetration of small molecules by their chemical constituents through thin films [25] and at the surface of thicker objects [26]. But in this case, the analysis is limited to a small, localized region and is incapable of making a bulk characterization of plasticization in polymer samples. Nonlinear ultrasonic testing has been shown as a promising technique to evaluate the penetration of small molecules in polyethylene, give a bulk assessment of internal stresses and modifications to the semi-crystalline structure of HDPE by observing spectroscopic variations [27].

In this paper, a newly developed non-destructive characterization technique based on nonlinear ultrasonics is compared to gravimetric and mechanical analyses to study the effects of biodiesel on different grades of polyethylene. The plasticizing ability of biodiesel will be studied relative to toluene, as a known plasticizer and will consider the impact of biodiesel ageing. The study results are meant to improve material compatibility libraries for part design involving exposure to this new biofuel.

## 3.2. Materials and methods

### 3.2.1. Materials

Four grades of polyethylene covering a wide range of properties were used. Three of the resins were HDPE grades, denoted with the prefix HD, while the fourth resin was a linear low density (LLDPE) grade, denoted with the prefix LL. The numbers after each prefix (HD and LL) refer to the polyethylene grade named by the vendor. The materials were provided by Imperial Oil Ltd (Sarnia, ON) in pellet form. A summary of properties can be found in Table 3.1, with data provided from the supplier. The polymer pellets were compression molded according to Procedure C of Annex 1 in ASTM D4703 and were cut into rectangular strips of dimensions 125 mm x 20 mm x 3 mm (thickness) for absorption and tensile tests.

**Table 3.1**. Summary of key properties of all resins used in the experimental work.

| Reference Code | Density (g/cm$^3$) | MFI (g/10min)* |
|---|---|---|
| **HD 8660.29** | 0.941 | 2.0 |
| **LL 8460.29** | 0.938 | 3.3 |
| **HD 6605.70** | 0.948 | 5.0 |
| **HD 6719.17** | 0.952 | 19 |

* MFI = melt flow index, measured according to ASTM D1238.

Biodiesel, a tallow-based methyl ester prepared from animal renderings, was generously provided by Rothsay Biodiesel Inc (Guelph, ON) in pure form (B100). The biodiesel was stored in a deep freezer at a temperature of -40 ºC till used for testing. The mentioned degraded biodiesel in the study was obtained by accelerated oxidation, heating it at 50 ℃ for 45 days immediately prior to testing. Toluene was obtained from Caledon Laboratories (ON, Canada).

### 3.2.2. Preparation of plasticized samples

Rectangular-cut specimens of each resin grade were placed in a test tube with fresh or degraded biodiesel and placed in a hot water bath (VWR Corporation) at 50 ºC for up to 45 days and their weights were measured daily to track the diffusion of biodiesel in to the samples. Fluid absorption was measured gravimetrically for three replicates of each grade with a Mettler Toledo AE200 Analytical Balance. Surfaces were wiped (dried) using paper towels before the measurements were taken. The concentration of absorbed biodiesel in the samples was given as a percent increase in mass. As a means of comparison, the same grades of polyethylene were also plasticized with toluene. With higher sorption properties in polyethylene, samples only needed to be prepared at 25 $^{o}$C with toluene to reach comparable uptake concentrations to those achieved with biodiesel for the subsequent analysis of properties.

### 3.2.3. Mechanical properties

Tensile tests were performed on notched rectangular strips. For the rectangular samples, two side notches of 2 mm depth were applied along the center-line using single-side sharped razor blades (VWR Corporation). Tests were executed in a universal mechanical testing system (Instron Corporation Model 3366) with a 5 kN load cell, at a cross-head speed of 35 mm/min. Results from tensile tests were based on three samples for each grades tested.

### 3.2.4. Ultrasonic testing

A physical non-destructive characterization of the plasticized samples was done through nonlinear ultrasonic testing. The following procedure was described in previous work [27]. Two ultrasonic transducers (Physical Acoustic Corporation, NJ) were coupled to the surface of the specimen using high vacuum grease (Dow Corning), with a center-to-center separation of 35 mm. The emitter (model R15) had a resonant frequency at 150 kHz whereas a broadband sensor (model F30a) was used for the receiver. Emitted ultrasonic pulses were produced at frequencies from 135 to 165 kHz in 1 kHz step increments, with the corresponding received signals recorded at an acquisition rate of 4 MHz and processed using a combination of a LabView and Python codes. A nonlinear ‘ultrasonic parameter’ was calculated from the ratio between the amplitude of third harmonic peak ($A_3$) over the amplitude at the primary emitted frequency ($A_1$).

### 3.2.5. Biodiesel characterization

The acid number was determined following ASTM D974 to track the extent of oxidation in the degrading fuel. For good sensitivity at low acidity values, a 0.01 N standardized KOH solution (Sigma-Aldrich) was used for the titrations. The endpoint was detected using phenolphthalein as an indicator. Tests were done in triplicates.

Surface tension was measured for pure fresh and pure degraded biodiesel using the pendant drop method by means of a 90º blunt end tip needle with a diameter of 1.27 mm. Twenty-six images, spaced 2 seconds apart, were taken for each drop by a digital camera acting as a goniometer and processed for their shape using an image analysis software (Kruss).

Viscosity of the fresh and degraded biodiesel was measured using a Discovery DHR-2 parallel plate rheometer (TA Instruments). A frequency sweep spanning 0.1–200 rad/s was performed at a temperature of 25℃ with a resolution of 5 points per decade. A Newtonian fit curve was provided at the end of the test, which was used to compute the viscosity of the biodiesel samples. The test was completed for three replicates of each fluid.

## 3.3. Results and discussion

### 3.3.1. Differences in absorption between biodiesel and toluene

In the preparation of biodiesel plasticized polyethylene specimens, their weight gains were monitored to assess absorption rate differences as well as final uptake between the different grades of polyethylene. Figure 3.1 shows the typical percent weight gain for the four polyethylene grades plotted against immersion time in fresh B100 biodiesel.

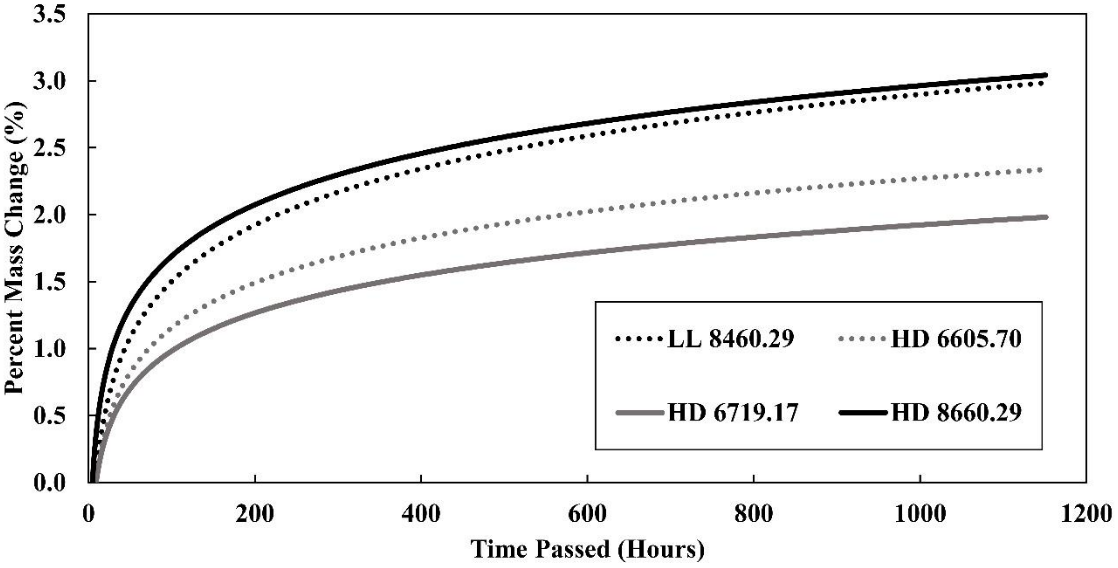

**Figure 3.1.** A plot of average percent weight change (%) vs. time passed (hours) in biodiesel of HD 8660.29 (black solid line), LL 8460.29 (black dotted line), HD 6605.70 (gray dashed line), and HD 6719.17 samples (gray solid line). Experimental data points were fitted with a logarithmic curve. The logarithmic curves were picked as they best represented the initial stages of the diffusion. The average $R^2$ value for all four grades is 0.73 depicting a good correlation.

The curves indicate that the samples had not fully equilibrated after 45 days but the trends shown suggest little further weight gains would be expected. Visual examination of the polymer samples after immersion showed distinctive yellow staining in comparison to their white appearance originally or after immersion in toluene. Faster absorption and ultimately greater fuel uptake was seen with the lower crystallinity/lower density polyethylene grades. HD 8660.29 showed a percent mass gain of approximately 3.04±0.07% over 45 days of immersion, followed by LL 8460.29 (2.98±0.02%), HD 6605.70 (2.34±0.03%) and finally HD 6719.17 with the lowest percent mass gain of approximately 1.98±0.01%; the lower densities associated with HD 8660.29 (0.941 g/cm$^3$) and LL 8460.29 (0.938 g/cm$^3$) in comparison to the other two grades exemplifies their lower crystallinity. Estimated diffusivity coefficients for a one-dimensional finite slab model (given in Table 3.2) were obtained by fitting the weight gain data to a simple but accurate approximation ($\pm$ 1%) of Equation 1, below [28]:

$$\frac{M_t}{M_\infty} = 1 - \frac{8}{\pi^2}\sum_{n=0}^{\infty}\frac{1}{(2n+1)^2}\exp\left(\frac{-D(2n+1)^2\pi^2 t}{l^2}\right) \tag{1}$$

where $M_t$ represents the mass uptake of biodiesel into the polyethylene slab up to time $t$; $M_\infty$ denotes the equilibrium mass uptake; $D$ is the diffusivity coefficient; and $l$ is the thickness of the slab. The approximation to this model, shown in Equation 2 below, for the early stages of the diffusion process (when less than 60% of biodiesel has diffused into the samples) was done with the assumption that the polymer strips are very thin and that diffusion of biodiesel through the edges can be neglected.

$$\frac{M_t}{M_\infty} = 4\left(\sqrt{\frac{Dt}{\pi l^2}}\right), for\ 0 < \frac{M_t}{M_\infty} < 0.6 \qquad (2)$$

The following approximation was chosen since it is a good illustration of the logarithmic curves (Figure 3.1) that provide a more adequate representation of the fitted weight gain data during the early stages of diffusion. Comparing diffusivity coefficients to the density of each polymer grade (given in Table 3.1), it appears that an inverse correlation exists.

**Table 3.2.** Diffusivity coefficients for biodiesel and toluene in LL 8460.29, HD 8660.29, HD 6605.70, and HD 6719.17.

| **Sample** | **Diffusivity of Samples in Biodiesel at 50°C [$\frac{m^2}{hours}$]** | **Diffusivity of Samples in Toluene at 25°C [$\frac{m^2}{hours}$]** |
|---|---|---|
| **HD 8660.29** | $(17.8 \cdot 10^{-10}) \pm (0.566 \cdot 10^{-10})$ | $(1.97 \cdot 10^{-6}) \pm (0.673 \cdot 10^{-6})$ |
| **LL 8460.29** | $(14.0 \cdot 10^{-10}) \pm (0.702 \cdot 10^{-10})$ | $(2.40 \cdot 10^{-6}) \pm (0.436 \cdot 10^{-6})$ |
| **HD 6605.70** | $(9.74 \cdot 10^{-10}) \pm (1.04 \cdot 10^{-10})$ | $(1.73 \cdot 10^{-6}) \pm (0.196 \cdot 10^{-6})$ |
| **HD 6719.17** | $(9.21 \cdot 10^{-10}) \pm (0.938 \cdot 10^{-10})$ | $(1.74 \cdot 10^{-6}) \pm (0.192 \cdot 10^{-6})$ |

The lower density grades, LL 8460.29 and HD 8660.29, have fitted coefficients approximately 30-45% higher than the higher density grades (HD 6605.70 and HD 6719.17), depicting a higher rate of diffusion of biodiesel into these polyethylene grades. In terms according to Cohen and Turnbull theory [4, 29], the higher diffusivity coefficient arises in LL 8460.29 and HD 8660.29 (Table 3.2) due to their larger free volume ($V_f$) on account of their greater amorphous content in comparison to HD 6605.70 and HD 6719.17. In other words, PE grades with higher crystalline content were less permeable to the diffusion of biodiesel, presenting a more tortuous path for the absorbed biofuel to accumulate in the amorphous regions of the polymer.

In order to compare plasticizing properties under mechanical and acoustic testing, samples were also prepared with a known plasticizer, toluene, which is a smaller molecule than biodiesel. To achieve a similar mass gain, immersion of polyethylene samples in toluene had to be done at a lower temperature in order to prevent samples from being distorted (data not shown); despite the lower ambient temperature (25 $^{o}$C), its absorption rates in Table 3.2 were faster than found for biodiesel at 50 $^{o}$C. The estimated diffusivity coefficients for toluene with all PE grades, included in Table 3.2, showed a similar trend but with values more than a 100% larger than those with biodiesel, depicting a much faster absorption rate into the samples. The final uptake of toluene for the different grades was highest for LL 8460.29 (4.27±0.39%). HD 8660.29 (3.83±0.23%) had a final uptake amount that is approximately 11% lower than LL 8460.29, HD 6605.70 (2.99±0.03%) and HD 6719.19 (3.07±0.08%) were approximately 43% and 39% lower, respectively. As seen by the values, the final uptake of toluene was slightly different among the grades compared to biodiesel uptake, though the larger difference due to density was consistent. This difference was due to the higher diffusion rate of toluene; and the focus of this test is to reach the closest comparable uptake of solvents for material characterization rather than finding the final equilibrium value.

### 3.3.2. Plasticization observed by traditional and nondestructive methods

Figure 3.2 shows the influence of the absorbed biodiesel and toluene on the mechanical properties of the polyethylene grades, following a traditional method for quantifying plasticization.

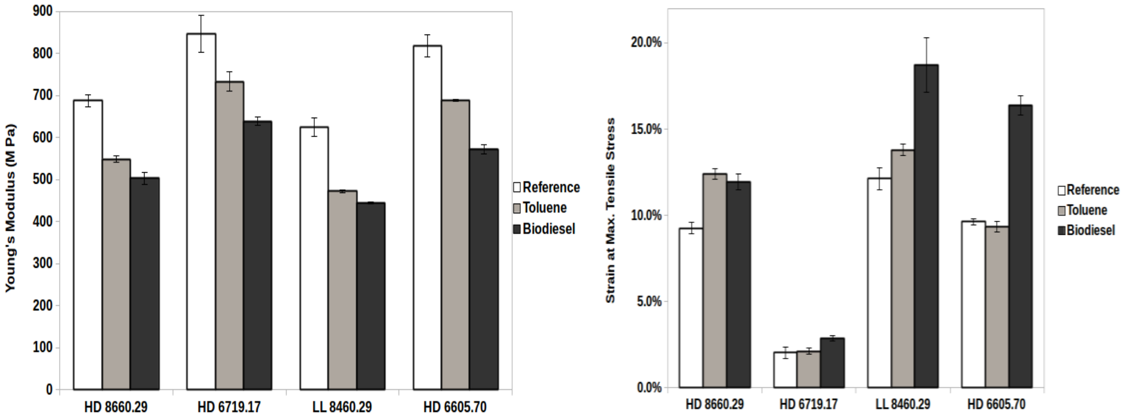

**Figure 3.2. a)** (Left) Summary of the elastic modulus of grades HD 8660.29, HD 6719.17, LL 8460.29, and HD 6605.70 in reference (white), toluene after 7 hours immersion (gray), and biodiesel after 45 days immersion (black). Error bars represent the standard deviation of the three samples tested for each grade. **b)** (Right) Summary of the strain at max stress of grades HD 8660.29, HD 6719.17, LL 8460.29, and HD 6605.70 in reference (white), toluene after 7 hours immersion (gray), and biodiesel after 45 days immersion (black). Error bars represent the standard deviation of the three samples tested for each grade.

The properties shown include Young's modulus and the strain-at-max stress of all polyethylene grades, respectively. The decline in modulus, for both fluids, shows that biodiesel shared attributes of a plasticizer in polyethylene, increasing chain mobility and reducing the secondary forces such as hydrogen bonding and Van der Waals forces between polymer chains [30]. The results show that the extent of change in mechanical properties by biodiesel is proportional to the amount of mass uptake. Samples with higher mass uptake (HD 8660.29 and LL 8460.29), showed a larger reduction in Young's modulus and greater increase in the strain at max stress. It is known that free volume possesses an inverse relationship with the rigidity of the polymer. Hence, as the free volume of the polymer is increased with increasing plasticizer concentration, the mobility of the polymer molecules also increases, making the polymer rubbery and soft. This loss of rigidity and increase in mobility is witnessed by the decrease in the elastic modulus and the increase in the strain at max stress.

In the face of differing absorbed content in the polymer at the time of the mechanical testing, a model was necessary to compare the plasticizing influence of biodiesel to toluene on polyethylene. The model of Sothornvit and Krochta [31] was chosen to compare and quantify the effects of plasticizer composition, size, and shape on the mechanical properties of a sample. They reported being able to successfully consider three different approaches to quantify the plasticizing influence and in all cases, found an exponential dependency on the elastic modulus ($EM$):

$$EM = EM_0 \cdot e^{-x \cdot k_{EM}} \qquad (2)$$

where $EM_0$ value reflects the original modulus of the polymer in the absence of a plasticizer; $k_{EM}$ (unitless) reflects the plasticizing efficiency of a penetrant; and $x$ is the plasticizer content ($x = \frac{(final\ mass\ of\ PE\ sample\ after\ immersion)-(inital\ mass\ of\ PE\ sample)}{(initial\ mass\ of\ PE\ sample)}$).

The first approach of Sothornvit and Krochta was used in this study, quantifying the change in modulus based on the mass of absorbed plasticizer per mass of PE sample, while the second and third approach, which were not used here, considered a molar basis of plasticizer per mole of PE or moles of oxygen atoms in the plasticizer per mole of PE, respectively. Table 3.3 shows the plasticizer efficiency, determined on a mass basis, for biodiesel versus toluene averaged for the four grades of polyethylene. As seen in the table, $k_{EM}$ for biodiesel was twice the value for toluene, indicating that biodiesel was more efficient as a plasticizer for polyethylene.

**Table 3.3.** Plasticizer efficiency of biodiesel versus toluene averaged for the four grades of polyethylene.

| $\boldsymbol{k_{EM}}$ **(Biodiesel)** | $\boldsymbol{k_{EM}}$ **(Toluene)** |
|---|---|
| $10.75 \pm 1.66$ | $5.73 \pm 0.66$ |

Although biodiesel demonstrated plasticization properties by traditional means of mechanical testing, the analysis using ultrasound indicated that its modes of interaction with the semi-crystalline structure of polyethylene are uniquely different from a plasticizer like toluene. Figures 3.3 and 3.4 show the different acoustic spectra attained from samples before and after immersion in biodiesel and toluene, respectively, where the weight gains were similarly around 2-4%.

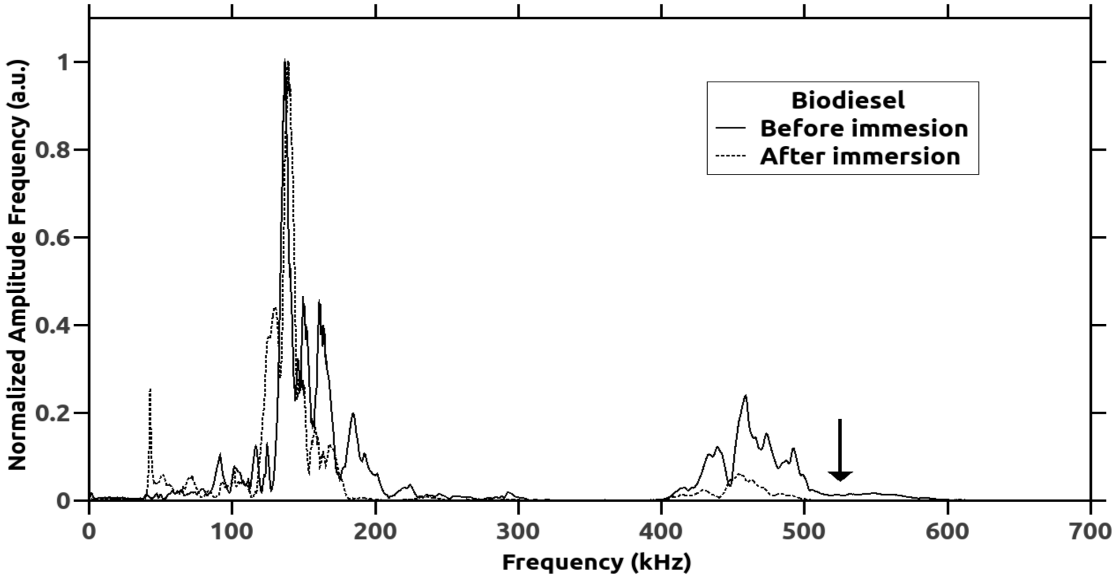

**Figure 3.3.** Ultrasonic spectra for the HD 8660.29 sample before and after biodiesel immersion (the arrow indicates the decrease of the third harmonic peak amplitude considering normalized signal based on primary frequency amplitude).

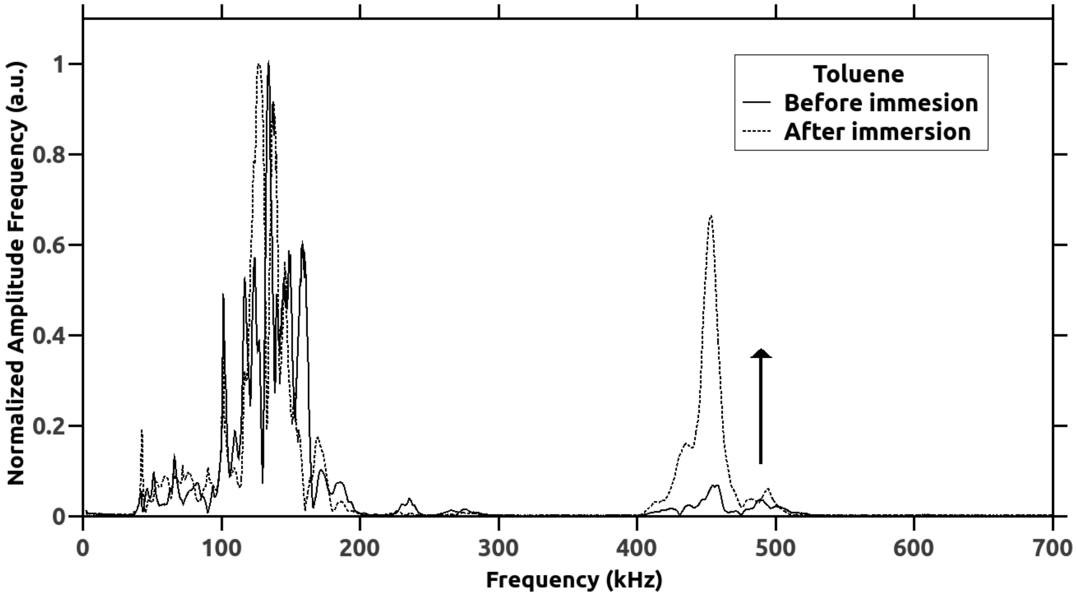

**Figure 3.4.** Ultrasonic spectra for the HD 8660.29 sample before and after toluene immersion (the arrow indicates the increase of the third harmonic peak amplitude considering normalized signal based on primary frequency amplitude).

The primary assumption of this analysis is that propagation of ultrasonic waves in PE will be dispersive, thus, presence of higher order harmonics will be detected. Unlike a perfect elastic body, propagation of these ultrasonic waves through a microstructure with discontinuities, such as those created in the semi-crystalline network with the penetration of solvents [27], can generate peaks at frequencies different from the original wave introduced. Experimental evidence has demonstrated that the observed harmonics is directly related with presence of non-linearities introduced in the structure of the material [32]. A distinct generation of third harmonic region (A3 – between 400-500 kHz) is observed in Figures 3.3 and 3.4. Second order and other higher order harmonic peaks were attenuated and thus not used for analysis. A descriptor used to quantify this difference is the amplitude ratio between the peaks of third harmonic (A3) and primary input frequency (A1), referred to as the ultrasonic parameter in this work. Variations in these ultrasonic parameters are connected with structural changes that interfere with the nonlinear propagation of the ultrasonic waves. For PE plasticized by toluene, this region presented a significant increase in the ultrasonic parameter through an increase in the amplitude of the third harmonic region ($A_3$), while biodiesel caused a minor reduction (shown by the arrows in Figures 3.3 and 3.4). The changes in the ultrasonic parameter for all the samples following immersion in toluene and biodiesel were computed and plotted in Figure 3.5.

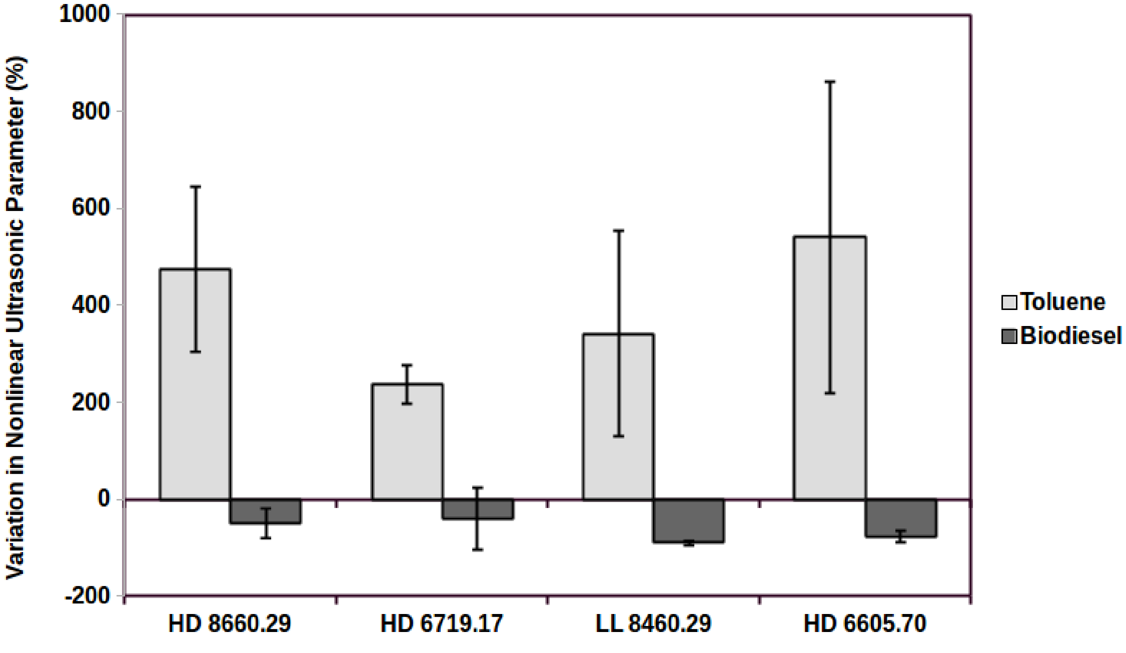

**Figure 3.5**. Nonlinear ultrasonic parameter variation for HD 8660.29, HD 6719.17, LL 8460.29, and HD 6605.70 with immersion in toluene and biodiesel.

When comparing the differences in the ultrasonic parameter, it is seen that the opposite behaviors in the third harmonics due to the influence of toluene or biodiesel was evident among all PE grades, with only a small difference attributed to crystallinity of the sample.

The interlamellar crystalline regions of the polymer samples are concentrated with stress transmitters spanning across the crystal lamellae boundaries, known as tie chains, which are associated with the mobility of the macromolecular network. These inter-crystalline regions can be affected by the penetration of low molecular weight contacting fluids, swelling the amorphous phase for polyethylene, and promoting internal stresses [33, 34]. The increase in the nonlinear ultrasonic parameter occurred in response to increasing internal stress forces created by the penetrating molecules. Conversely, the decline in the nonlinear ultrasonic parameter shown in Figures 3.3 and 3.4, due to biodiesel absorption, is related to a relative decrease in internal stresses. This argument can be connected to observations of the necking regions during mechanical testing of these polyethylene samples after their immersion in the different plasticizers. Samples exposed to biodiesel exhibited a significant decrease in fibrillation while being stretched compared to those exposed to toluene. The absorbed biodiesel lubricated the inter-crystalline chains, similar to a stress-cracking agent, promoting crystal slippage during plastic deformation with no increase in internal stress. This was an interesting finding as it indicated the acoustic technique was differentiating the function of these two fluids with polyethylene in a manner not detectable by mechanical testing.

### 3.3.3. Effects of degradation of biodiesel on plasticization

Oxidative degradation of biodiesel results in chemical and physical changes to its properties, notable in its varying hydrophobicity and color, which may affect its absorption into polyethylene. Figure 3.6 presents the percent weight gains plotted against the time, from immersion in previously degraded biodiesel.

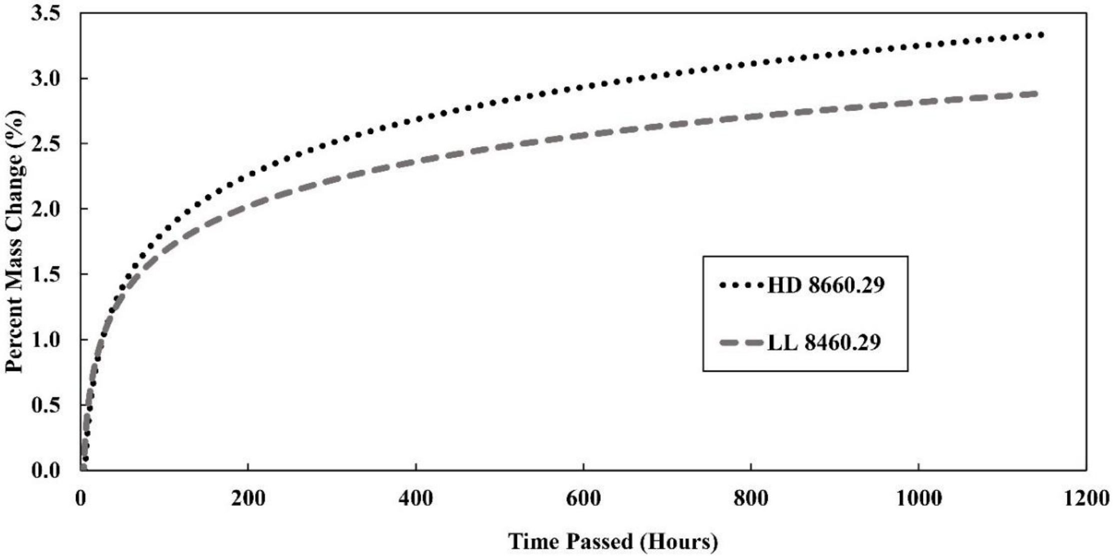

**Figure 3.6.** Plot of average percent weight change (%) vs. time passed (hours) of HD 8660.29 in degraded biodiesel (black dotted line), and LL 8460.29 in degraded biodiesel (gray dashed line). Experimental data points were fitted with a logarithmic curve. Experimental data points were fitted with a logarithmic curve. The average $R^2$ value for the two grades is 0.83 depicting a good correlation.

The plot shows no differences in the diffusion mechanism compared to fresh biodiesel (Figure 3.1) but the absorption rate was slightly lower with the degraded biofuel for LL 8460.29 and slightly higher for HD 8660.29. The LL 8460.29 samples in degraded biodiesel exhibited a percent mass change (2.89±0.06%) that was only 3.0% lower than fresh biodiesel whereas for the HD 8660.29 samples, the percent mass change (3.33±0.10%) was 9.53% lower.

The continued progression in oxidation during the immersion trials with both fresh biodiesel (Figure 3.1) and degraded biodiesel (Figure 3.6) was followed by determining the acid number and viscosity of the fluids over time; one must recognize that a fresh biodiesel sample experienced degradation as well in any such ageing studies since the antioxidants present in a commercial fuel will be consumed relatively quickly at 50 $^{o}$C. Figure 3.7 shows the acid number of both the degraded biodiesel and fresh biodiesel over time, reflecting changes in the concentration of acid groups formed as by-products of biodiesel ageing.

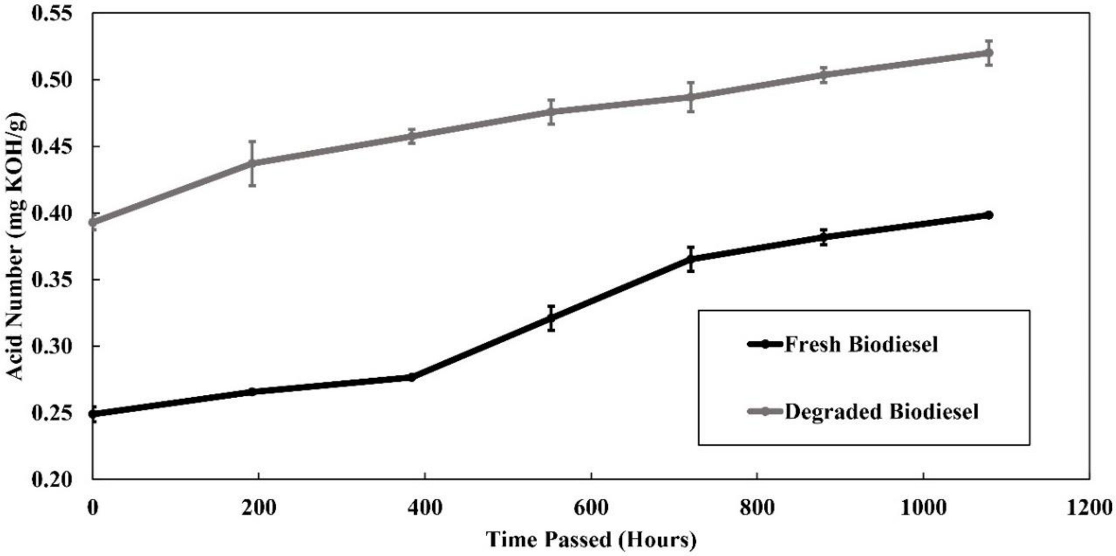

**Figure 3.7.** Plot of acid value vs. time passed for fresh biodiesel (black solid line) and degraded biodiesel (gray dashed line). Standard deviations, shown by the error bars, were higher with the degraded biodiesel due to the darker color making it more difficult to see the end point.

The two biofuels showed an ‘almost constant’ rate of increase in acid number even though the previously degraded biodiesel was always higher in value. The surface tension of fresh biodiesel, measured at Day 0, (25.95 ± 0.41 mN/m) was found to change very little from the 45-day degraded biodiesel (23.90 ± 0.34 mN/m). Acid groups were being increased in the fuel but the complex set of oxidation products related to degradation [34] meant the overall hydrophilicity was unchanged. On the other hand, the viscosity measurements showed no significant changes in the viscosity of biodiesel over the degradation time, for either case, and consequently the data was not presented in the paper.

Mechanical testing found no significant differences between polyethylene samples plasticized by fresh versus degraded biodiesel, in terms of Young's Modulus or strain-at-max stress for both LL 8460.29 and HD 8660.29. The differences in biodiesel uptake between the fresh and degraded biodiesel were too small to have a detectable effect on the mechanical properties of the samples. Using Equation 2, the plasticization efficiency ($k_{EM}$) of the degraded biodiesel was found to be equal to $11.86 \pm 1.35$, which is not significantly different from that of fresh biodiesel ($10.75 \pm 1.66$). In comparison, Figure 3.8 presents the variation of the nonlinear ultrasonic parameter for samples that were immersed in either fresh and degraded biodiesel.

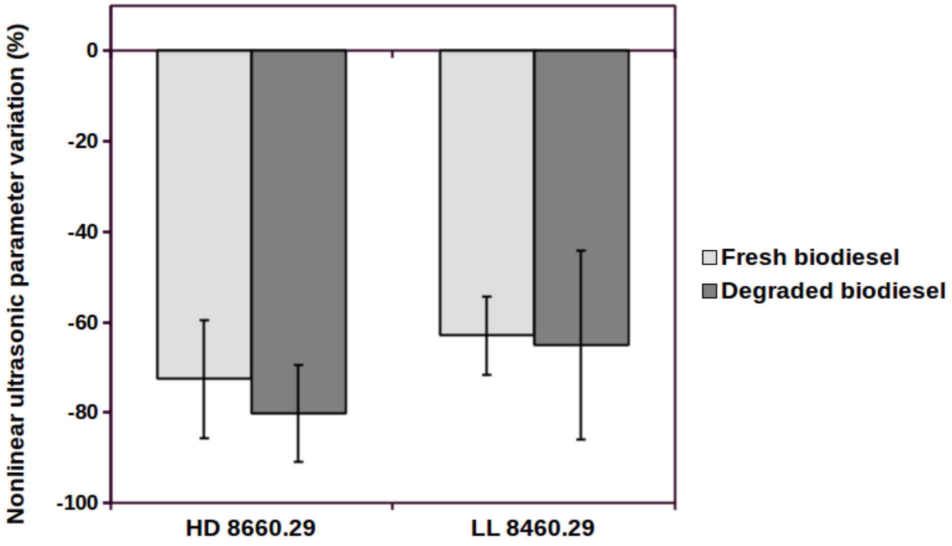

**Figure 3.8**. Nonlinear ultrasonic parameter variation for HD 8660.29 and LL 8460.29 with immersion in fresh and degraded biodiesel.

The results show that all samples experienced the same decrease in the variation of ultrasonic parameter after immersion but differences were too small to consider the degraded biofuel to be affecting polyethylene differently. Since no significant difference was observed in both mechanical and ultrasonic tests, one concludes similar compatibility when using fresh and degraded biodiesel with polyethylene.

## 3.4. Conclusions

The compatibility assessment of biodiesel with polyethylene for use in fuel-contact service revealed a plasticizing property, though not as a swelling agent. Results from gravimetric analysis have noted a higher diffusivity coefficient (i.e. higher penetration rate) for biodiesel in polyethylene samples of lower density (i.e. lower crystallinity). Immersion of the same samples in toluene showed a slightly different absorption behavior and higher diffusion rates in comparison to biodiesel. The effect of biodiesel and toluene sorption on the mechanical properties (Young's Modulus) of polyethylene showed significantly higher plasticization efficiencies for biodiesel in comparison to toluene. A novel non-destructive testing method based on ultrasonics was used to evaluate biodiesel plasticization (in comparison to toluene). Differences in the resulting acoustic signature expressed by biodiesel and toluene revealed interesting evidence of different modes of interaction (plasticization) with the semi-crystalline structure of polyethylene between the two fluids, that was not detectable by the mechanical testing. An increase in the nonlinear ultrasonic parameter is witnessed by the toluene plasticized samples as a result of increasing internal stress forces created by the penetrating molecules. Conversely, a decline in the nonlinear ultrasonic parameter is witnessed in the biodiesel plasticized samples in relation to a relative decrease in internal stresses. Oxidation of biodiesel by degradation was found to only slightly affect the diffusion rate of biodiesel into polyethylene samples, though mechanical and ultrasonic testing showed no significant differences in the plasticization capability of biodiesel.

Future studies by our group will concentrate on attaining a deeper understanding of the compatibility of biodiesel and polyethylene, specifically the accelerated failures that can occur upon exposure of the small stresses.

## Acknowledgements

The authors would like to thank Imperial Oil Ltd., Natural Sciences and Engineering Research Council (NSERC), and the Conselho Nacional de Desenvolvimento Científico e Tecnológico (CNPq) for funding the work. The authors would like to especially thank Ron Cooke at Imperial Oil for his advice, supply of materials, and technical insights.

# References

[1] O.-G. Piringer, A.L. Baner, Plastic packaging: interactions with food and pharmaceuticals, Wiley-VCH, Weinheim, 2008.

[2] W. Trakarnpruk, S. Porntangjitlikit, Palm oil biodiesel synthesized with potassium loaded calcined hydrotalcite and effect of biodiesel blend on elastomer properties, Renewable Energy. 33 (2008) 1558–1563. doi:10.1016/j.renene.2007.08.003.

[3] B. Flitney, Which elastomer seal materials are suitable for use in biofuels?, Sealing Technology. 2007 (2007) 8–11. doi:10.1016/s1350-4789(07)70409-9.

[4] E. Richaud, Flaconnèche Bruno, J. Verdu, Biodiesel permeability in polyethylene, Polymer Testing. 31 (2012) 170–1076. doi:10.1063/1.4738433.

[5] M. Böhning, U. Niebergall, A. Adam, W. Stark, Influence of biodiesel sorption on temperature-dependent impact properties of polyethylene, Polymer Testing. 40 (2014) 133–142. doi:10.1016/j.polymertesting.2014.09.001.

[6] M. Schilling, M. Böhning, H. Oehler, I. Alig, U. Niebergall, Environmental stress cracking of polyethylene high density (PE-HD) induced by liquid media - Validation and verification of the full-notch creep test (FNCT), Materialwissenschaft Und Werkstofftechnik. 48 (2017) 846–854. doi:10.1002/mawe.201700065.

[7] M.M. Maru, M.M. Lucchese, C. Legnani, W.G. Quirino, A. Balbo, I.B. Aranha, et al., Biodiesel compatibility with carbon steel and HDPE parts, Fuel Processing Technology. 90 (2009) 1175–1182. doi:10.1016/j.fuproc.2009.05.014.

[8] M. Böhning, U. Niebergall, A. Adam, W. Stark, Impact of biodiesel sorption on mechanical properties of polyethylene, Polymer Testing. 34 (2013) 17–24. doi:10.1016/j.polymertesting.2013.12.003.

[9] M. Böhning, U. Niebergall, M. Zanotto, V. Wachtendorf, Impact of biodiesel sorption on tensile properties of PE-HD for container applications, Polymer Testing. 50 (2016) 315–324. doi:10.1016/j.polymertesting.2016.01.025.

[10] M. Weltschev, J. Werner, M. Haufe, M. Heyer, Compatibility of High-Density Polyethylene Grades with Biofuels, Packaging Technology and Science. 27 (2013) 231–240. doi:10.1002/pts.2028.

[11] M. Thompson, B. Mu, C. Ewaschuk, Y. Cai, K. Oxby, J. Vlachopoulos, Long term storage of biodiesel/petrol diesel blends in polyethylene fuel tanks, Fuel. 108 (2013) 771–779. doi:10.1016/j.fuel.2013.02.040.

[12] G. Lutz, J.F. Mata-Segreda, Kinetics of interaction of palm ethyl biodiesel with three different polymer materials, Journal of Physical Organic Chemistry. 21 (2008) 1068–1071. doi:10.1002/poc.1427.

[13] H.J. Nieschlag, I.A. Wolff, Industrial uses of high erucic oils, Journal of the American Oil Chemists Society. 48 (1971) 723–727. doi:10.1007/BF02638529

[14] P.P. Kundu, Improvement of filler-rubber interaction by the coupling action of vegetable oil in carbon black reinforced rubber, Journal of Applied Polymer Science. 75 (1999) 735–739. doi:10.1002/(sici)1097-4628(20000207)75:6<735::aid-app1>3.0.co;2-t.

[15] V. Nandanan, R. Joseph, K.E. George, Rubber seed oil: A multipurpose additive in NR and SBR compounds, Journal of Applied Polymer Science. 72 (1999) 487–492. doi:10.1002/(sici)1097-4628(19990425)72:4<487::aid-app4>3.0.co;2-m.

[16] J. Wehlmann, Use of esterified rapeseed oil as plasticizer in plastics processing, Lipid - Fett. 101 (1999) 249–256. doi:10.1002/(sici)1521-4133(199907)101:7<249::aid-lipi249>3.0.co;2-i.

[17] F. Cataldo, O. Ursini, G. Angelini, Biodiesel as a Plasticizer of a SBR-Based Tire Tread Formulation, ISRN Polymer Science. 2013 (2013) 1–9. doi:10.1155/2013/340426.

[18] R. Mccormick, M. Ratcliff, L. Moens, R. Lawrence, Several factors affecting the stability of biodiesel in standard accelerated tests, Fuel Processing Technology. 88 (2007) 651–657. doi:10.1016/j.fuproc.2007.01.006.

[19] M. Fazal, A. Haseeb, H. Masjuki, Biodiesel feasibility study: An evaluation of material compatibility; performance; emission and engine durability, Renewable and Sustainable Energy Reviews. 15 (2011) 1314–1324. doi:10.1016/j.rser.2010.10.004.

[20] M. Jakeria, M. Fazal, A. Haseeb, Influence of different factors on the stability of biodiesel: A review, Renewable and Sustainable Energy Reviews. 30 (2014) 154–163. doi:10.1016/j.rser.2013.09.024.

[21] E. Richaud, B. Fayolle, J. Verdu, J. Rychlý, Co-oxidation kinetic model for the thermal oxidation of polyethylene-unsaturated substrate systems, Polymer Degradation and Stability. 98 (2013) 1081–1088. doi:10.1016/j.polymdegradstab.2013.01.008.

[22] E. Richaud, F. Djouani, B. Fayolle, J. Verdu, B. Flaconneche, New Insights in Polymer-Biofuels Interaction, Oil & Gas Science and Technology – Revue d'IFP Energies Nouvelles. 70 (2013) 317–333. doi:10.2516/ogst/2013151.

[23] N. Lützow, A. Tihminlioglu, R.P. Danner, J. Duda, A.D. Haan, G. Warnier, et al., Diffusion of toluene and n-heptane in polyethylenes of different crystallinity, Polymer. 40 (1999) 2797–2803. doi:10.1016/s0032-3861(98)00473-x.

[24] R. Kwamen, B. Blümich, A. Adams, Estimation of Self-Diffusion Coefficients of Small Penetrants in Semicrystalline Polymers Using Single-Sided NMR, Macromolecular Rapid Communications. 33 (2012) 943–947. doi:10.1002/marc.201100847.

[25] D. Cava, R. Catala, R. Gavara, J.M. Lagaron, Testing limonene diffusion through food contact polyethylene by FT-IR spectroscopy: Film thickness, permeant concentration and outer medium effects, Polymer Testing. 24 (2005) 483–489. doi:10.1016/j.polymertesting.2004.12.003.

[26] M. Wang, P. Wu, S.S. Sengupta, B.I. Chadhary, J.M. Cogen, B. Li, Investigation of Water Diffusion in Low-Density Polyethylene by Attenuated Total Reflectance Fourier Transform Infrared Spectroscopy and Two-Dimensional Correlation Analysis, Industrial & Engineering Chemistry Research. 50 (2011) 6447–6454. doi:10.1021/ie102221a.

[27] F. Gomes, W. West, M. Thompson, Effects of annealing and swelling to initial plastic deformation of polyethylene probed by nonlinear ultrasonic guided waves, Polymer. 131 (2017) 160–168. doi:10.1016/j.polymer.2017.10.041.

[28] Fundamentals and applications of controlled release drug delivery, Springer, Place of publication not identified, 2014.

[29] M.H. Cohen, D. Turnbull, Molecular Transport in Liquids and Glasses, The Journal of Chemical Physics. 31 (1959) 1164–1169. doi:10.1063/1.1730566.

[30] M. Bocqué, C. Voirin, V. Lapinte, S. Caillol, J.-J. Robin, Petro-based and bio-based plasticizers: Chemical structures to plasticizing properties, Journal of Polymer Science Part A: Polymer Chemistry. 54 (2015) 11–33. doi:10.1002/pola.27917.

[31] R. Sothornvit, J.M. Krochta, Plasticizer effect on mechanical properties of β-lactoglobulin films, Journal of Food Engineering. 50 (2001) 149–155. doi:10.1016/s0260-8774(00)00237-5.

[32] C.J. Lissenden, Y. Liu, J.L. Rose, Use of non-linear ultrasonic guided waves for early damage detection, Insight - Non-Destructive Testing and Condition Monitoring. 57 (2015) 206–211. doi:10.1784/insi.2015.57.4.206.

[33] A. Krajenta, A. Rozanski, R. Idczak, Morphology and properties alterations in cavitating and non-cavitating high density polyethylene, Polymer. 103 (2016) 353–364. doi:10.1016/j.polymer.2016.09.068.

[34] A. Rozanski, A. Galeski, Plastic yielding of semicrystalline polymers affected by amorphous phase, International Journal of Plasticity. 41 (2013) 14–29. doi:10.1016/j.ijplas.2012.07.008.

[35] N. Kumar, Oxidative stability of biodiesel: Causes, effects and prevention, Fuel. 190 (2017) 328–350. doi:10.1016/j.fuel.2016.11.001.

# Chapter

# 4. Studying the Mechanism of Biodiesel Acting as an Environmental Stress Cracking Agent with Polyethylenes

# Studying the mechanism of biodiesel acting as an environmental stress cracking agent with polyethylenes

A.K. Saad, H.A. Abdulhussain, F.P.C. Gomes, J. Vlachopoulos, M.R. Thompson*
Department of Chemical Engineering, CAPPA-D/MMRI
McMaster University, Hamilton, Ontario, Canada

Manuscript draft under review

## Author contributions:

The first author, A.K. Saad, was responsible for the design and execution of the experiments, and analysis of data. The author was also responsible for writing majority of the manuscript as well as submission and publishing of manuscript. The second author, H. A. Abulhussain, completed all additional edits for the ultrasonic code and provided help in execution of the experiments and writing of parts of the manuscript and revision of it. The third author, F. Gomes, was responsible for revision of the manuscript. The authors, M.R. Thompson and J. Vlachopoulos, were responsible for supervision of the design and completion of experiments as well as revision of the manuscript.

## Main scientific contributions of the paper:

- Use of a novel non-destructive testing method based on ultrasonics to investigate the effects of biodiesel as an environmental stress cracking agent for polyethylene.
- Proposal of a concentration limited plasticization mechanism for environmental stress cracking of polyethylene by biodiesel.
- Demonstration of the ability of biodiesel to interact with different grades of polyethylene as both an environmental stress cracking and a plasticizing agent.

## Abstract

This paper focuses on understanding the compatibility of biodiesel with different grades of polyethylene, specifically examining the environmental stress cracking ability of biodiesel. Traditional testing methods were used with a newly developed nondestructive ultrasonic testing method to investigate the different modes of interaction by biodiesel with this common polymer. Analysis showed that biodiesel exhibited attributes of both a stress cracking agent and a plasticizing agent, with the different modes contingent on the crystalline content and molecular weight of the polymer. Higher crystallinity and lower molecular weight polyethylenes showed a higher susceptibility to environmental stress cracking by this biofuel; while lower crystallinity and higher molecular weight polyethylenes were more likely to experience only plasticization. Gravimetric analysis, visual inspection, and infrared spectroscopy aided in monitoring fluid absorption into the notched specimens. When highly localized absorption occurred around the notch, the sample had a high tendency to fail in the presence of biodiesel; meanwhile samples experiencing absorption over the whole body were unlikely to crack. Combining the evidence observed in this study, a concentration-limited plasticization mechanism for environmental stress cracking by biodiesel was proposed with polyethylene and explained using the ultrasonic testing method that can help with early failure detection and material selection.

**Keywords:** Compatibility; Ultrasonic Testing; Igepal; Fourier-transform infrared spectroscopy.

## 4.1. Introduction

The relatively inert nature, along with other valuable properties, of polyethylene (PE) have without a doubt made it a prevalent material in today's world, with uses in numerous applications ranging from simple household items, such as recycling bins, to industrial applications such as the storage of chemicals including fuel tanks in automobiles, marine vessels, and agricultural machinery [1]. As a result, parts fabricated from PE are often exposed to aggressive environments that may cause chemical and physical changes leading to early failure if not properly selected for the use. Nearly 70 years ago, environmental stress cracking (ESC) was first identified in the polymer industry as a significant problem to be considered when selecting PE grades, especially for contact applications with fluids such as piping and tank fabrication [2-7]. An estimated 15-40% of all plastic component failures based on application can be traced to ESC [7,8]. Interestingly, the mechanism of ESC is still not completely understood despite the length of time since it was first recognized.

ESC relates to an accelerated brittle failure of a polymer, resulting from low-to-moderate stresses while in contact with fluids such as alcohols or detergents [9-16]. It is considered a physical phenomenon since the polymer chains are not chemically altered [17]. Failures related to ESC are believed to occur under very specific localized conditions related to chain morphology, absorbed concentration of the contacting fluid, and concentrated stresses producing this deleterious outcome. Several testing methods are available to characterize slow crack growth (SCG) and ESC, including the standardized full-notch creep test (FNCT) (ISO 16770) [18], the notched constant tensile load test

(NCTL) (ASTM D5397) [19], the Pennsylvania Notch Test (PENT) (ASTM F1473) [20], and the Bell Test (ASTM D1693) [21]. Ironically, the active fluids related to ESC often have little perceived influence on the polymer, which makes the phenomena all the more troubling to identify. The present study arose from concerns that biodiesel could be one such active fluid.

The depletion of fossil fuel reserves along with the environmental issues associated with using them has renewed interest in biodiesel as a substitute, making its application with PE to be an immediate compatibility concern when considering that many tanks are nowadays fabricated with this material [22]. Few studies of biodiesel with PE have been conducted to date [12,23-29], finding only weak evidence that chemical interactions can occur. In the face of some troubling early failures being reported to industry for parts contacting this biofuel, it seemed prudent to consider ESC as the likely cause. This is a new consideration for the polymer industry, with only two very recent studies to suggest that biodiesel could be an ESC agent [11,30]. The study by Schilling and Böhning [11] used detergents as characteristic model fluids for biodiesel and diesel to characterize ESC of different high density PEs by the two mediums. Their results showed the ESC ability of biodiesel through accelerated failure in comparison to air, but with lower aggressiveness than diesel. The lower ESC effect of biodiesel had been attributed to the slower absorption rate and lower final equilibrium concentration of biodiesel in PE. In our own studies examining biodiesel as a plasticizer for PE [30], a newly developed non-destructive characterization based on nonlinear ultrasonics for monitoring internal stresses [31] noted a phenomena more closely resembling interactions with other popular active fluids like IGEPAL rather than commonly recognized plasticizers for PE like toluene. This ultrasonic characterization tool has been utilized again in the present work to better understand the ESC mechanism of biodiesel with PE. In that study, we found the color of biodiesel showed its distribution in the polymer, leading to the hypothesis that a deeper study of the mechanism for ESC would be possible with this fluid.

Therefore, the current study intends to further research the possibility that biodiesel could be an ESC agent with PEs and based on its findings, propose a mechanism of interaction. The work uses the aforementioned nonlinear ultrasonic characterization method in conjunction with gravimetric analyses and infrared vibration spectroscopy (FT-IR) to monitor the time dependent progression of biodiesel into different grades of PE. The results are meant to aid our previous study in improving material compatibility libraries for parts design involving exposure of PE to this new biofuel.

## 4.2. Materials and methods

### 4.2.1. Materials

Four grades of high-density polyethylene (HDPE) covering a wide range of properties were used, picked based on their stress cracking ability. The materials were provided by Imperial Oil Ltd (Sarnia, ON) in pellet form. A summary of properties can be found in Table 4.1, with data provided from the supplier. The properties of the polymer grade LA 080 were not provided by the supplier, hence were found using suitable characterization methods. The polymer pellets were compression molded according to Procedure C of Annex 1 in ASTM D4703 and were machine cut into rectangular strips of dimensions 65 mm x 13 mm x 3 mm (thickness) for testing.

**Table 4.1.** Summary of key properties of all resins used in the experimental work.

| Reference Code | Density (g/cm$^3$) | MFI (g/10min) | ESCR ($F_{50}$ hours, IGEPAL) |
|---|---|---|---|
| **HD 6605.70** | 0.948 | 5.0 | 20 |
| **LA 080** | 0.934$^1$ | 0.3$^2$ | 47$^3$ |
| **HD 8660.29** | 0.941 | 2.0 | 40 |
| **HD 6908.19** | 0.965 | 8.2 | 3 |

1) ESCR = environmental stress cracking resistance.
2) Density was measured using a Mirage MD-200S Electronic Densimeter. Three dog bone samples were used for average value quoted.
3) MFI = melt flow index, measured according to ASTM D1238.
4) Values were determined using ASTM D1693 with 10% IGEPAL CA-630.

Biodiesel, a tallow-based methyl ester prepared from animal renderings, was generously provided by Rothsay Biodiesel Inc (Guelph, ON) in pure form (B100). The biodiesel was stored in a deep freezer at a temperature of -40 ºC till used for testing. IGEPAL CA630 (Nonylphenoxy poly(ethyleneoxy) ethanol) was obtained from Sigma Aldrich (Mississauga, ON); IGEPAL CA630 can be used as a substitute for CO630 in the

Bell Test [32]. Due to the limited supply of biodiesel available and since experimental results showed similar aggressiveness between a 10% biodiesel in aqueous solution and B100 biodiesel, the 10% solution was used for the majority of testing. IGEPAL was also used at a concentration of 10% in water at 50 ℃ (Condition A and B) to promote rapid failure and fairly short test times [21]. The low sulfur diesel (summer grade) used in some testing was obtained from Esso Ltd (Hamilton, ON), to make a 10% biodiesel solution in petroleum diesel.

### 4.2.2. Modification of the Bell Test

Standardized samples dictated by the Bell Test (ASTM D1693) were too short to provide sufficient surface area to affix the ultrasonic sensors when such analysis was conducted. Therefore, to overcome this issue, the length of the samples was modified, while maintaining all other dimensions (65 mm x 13mm x 3mm (thickness)), to allow simultaneous testing by ultrasonic analysis. The nicking jig used in the Bell Test was also modified to allow notching of the new sample sizes.

To reasonably ensure the same stresses were applied to the modified samples as in the original test, the radius of curvature (5.1 mm) of the bent samples was preserved. Modified u-shaped holders were made to fit one sample while maintaining the radius of curvature at 5.1 mm. This allowed us to perform ultrasonic testing on the samples, one at a time, without having to remove them from the holder, hence maintaining the applied stress throughout the experiment.

Each sample, held in its housing, was immersed in a sealed glass test tube containing the aqueous solution of 10% biodiesel and then placed in a heated circulating water bath (VWR Corporation) at 50 ºC till the sample failed or after 1000 hours of immersion time has passed. The solutions were agitated daily to ensure proper mixing and samples were taken out at documented times during the experiment for further analysis. After each of the analyses described below, at least until failure, the sample was placed back the glass tube and returned to the water bath. Each time the sample was removed lasted for approximately 20 minutes. A minimum of five samples were tested for each grade of PE.

A control group was run using the same procedure above on HD 6908.19 in water at 50℃. Since the HD 6908.19 samples cracked after approximately 4.73±0.40 hours in the aqueous solution with 10% biodiesel (ref. to Section 3.2), the control samples were left to age in water for an extended time of 7 hours.

### 4.2.3. Gravimetric analysis

The absorption of fluid into a sample was monitored gravimetrically at documented times with a Mettler Toledo AE200 Analytical Balance. The periodicity of testing was dependent on the ESCR of the polymer grade: for grade HD 6908.19, testing was done every hour; HD 6605.70 was tested every day; grades HD 8660.29 and LA 080 were tested every two days. The surface of a sample and its housing was wiped dry carefully using paper towels before weighing. The concentration of absorbed biodiesel in the samples was calculated based on percent mass gain.

### 4.2.4. Ultrasonic testing

To monitor structural effects caused by the biodiesel in PE over time without destroying the sample, a characterization developed based on nonlinear ultrasonic was done immediately following the gravimetric analysis. Following a similar procedure described in earlier work [31], two ultrasonic transducers (a resonant (R15a) and a broadband (F30a) sensor (Physical Acoustic Corporation) were affixed to the surface of the specimen using high vacuum grease (Dow Corning) at a center-to-center distance of approximately 30 mm. The emitter (R15a) has a resonant frequency at 150 kHz; whereas the receiver (F30a) has a flat frequency response over the range of 150 to 750 kHz. Ultrasonic guided waves were produced in a sample by pulse transmission at frequencies from 135 to 165 kHz in 1 kHz step increments produced with an Agilent 33210A waveform generator. The received signal was amplified using a Physical Acoustic 2/4/6c amplifier set to +40dB and collected at an acquisition rate of 4 MHz using a National Instruments 10 MHz 12-bit 4-channel data acquisition system. Each signal was converted to the frequency domain using a fast Fourier-transform. The frequency dependent amplitudes for all 31 spectra were averaged to get a single spectrum representing the response of a sample to the signals emitted. A nonlinear 'ultrasonic parameter' was calculated from the ratio between the amplitude of third harmonic peak ($A_3$) over the amplitude at the primary emitted frequency ($\mathbf{A_1}$); the frequency range of this higher harmonic was selected based on previously identified guided wave modes for the sample due to their low attenuation. To minimize errors brought about by ambient noises and the position of the sensors on the heterogenous morphology of each sample, the whole process was repeated four times for each reading and the results were averaged to attain a final ultrasonic parameter that is representative of the sample.

### 4.2.5. Infrared vibrational spectroscopy

Fourier-transform infrared spectroscopy (FT-IR) was performed with a Thermo Scientific Nicolet 6700 in attenuated total reflection (ATR) mode on samples at the beginning (before immersion in biodiesel solution) and end (after cracking in biodiesel solution/after 1000 hours of immersion) of the experiment. An average of 64 scans at a resolution of 0.4 $\mathrm{cm}^{-1}$ were reported for the mid-range wavenumbers (between 700 and 4000 $\mathrm{cm}^{-1}$). Post baseline correction, a Voigt window search was used to identify peaks. Due to the absence of a unique normalizing peak between biodiesel and PE, the resulting spectra were not normalized to avoid reduction of the actual peak height of biodiesel. Prior to testing using FT-IR, the samples were gently washed with de-ionized water and wiped to remove residual biodiesel.

In order to identify the depth of biodiesel diffusion at the notched region, a failed sample was separated into two halves and the exposed cross-sectional region at the crack was analyzed using a microtome (American Optical Corporation) to cut thin films perpendicular to the longitudinal axis. Each film was cut with a thickness of 100 μm and pressed against the ATR window for analysis. Similarly, the same analysis at the end of the specimen furthest from the notch/crack, again perpendicular to the longitudinal axis. When the samples that did not fail, the bent specimen was microtomed at the notch and at the end of the specimen.

### 4.2.6. Microscopic imaging

Optical images were taken using a Keyence vhx-5000 digital microscope. 5x and 50x lenses was used to obtain high quality digital pictures of a sample. Image of crack initiation was taken at the time when failure was first witnessed visually, whereas the image of the notch was taken after >1000 hours immersion in the aqueous biodiesel solution.

### 4.2.7. Crystalline characterization using Differential Scanning Calorimetry

Differential Scanning Calorimetry (DSC) was used to estimate the crystallinity content for each grade tested. DSC characterization was preformed using a Q2000 DSC from TA Instruments over a temperature range of -50 ℃ to 250 ℃ at a ramp rate of 10 ℃/min using nitrogen gas flow. Approximately 10 mg of each polymer grade was taken from the notched area and transferred into a Tzero non-hermetic aluminum pan covered with an aluminum lid for characterization. The percent crystallinity was calculated using Equation (1) below, based on the measured enthalpy and a theoretical heat of fusion for a 100% crystalline PE (293 J/g):

$$\%\ \mathrm{Crystallinity} = \frac{\Delta \mathrm{H}_{\mathrm{f}_{\mathrm{sample}}}}{\Delta \mathrm{H}_{\mathrm{f}_{100\%\ \mathrm{crystalline\ PE}}}} \times 100\% \tag{1}$$

where $\Delta \mathrm{H}_{\mathrm{f}_{\mathrm{sample}}}$ is the enthalpy of fusion of the sample; and $\Delta \mathrm{H}_{\mathrm{f}_{100\%\ \mathrm{crystalline\ PE}}}$ is the enthalpy of fusion for a 100% crystalline PE.

## 4.3. Results and discussion

### 4.3.1. Benchmarking biodiesel as a stress cracking agent

In order to establish biodiesel as an ESC agent for PE and to compare its aggressiveness to IGEPAL (a known ESC agent), samples of HD 6605.70 were tested against six different mediums: pure biodiesel (B100), an aqueous solution of 10% biodiesel, 10% biodiesel in petroleum diesel (B10 solution), an aqueous solution of 10% IGEPAL, water, and air. Samples in B100, B10, and the aqueous solution with 10% biodiesel cracked after 13 days, depicting comparable aggressiveness between the three mediums, while the baseline samples in water and air cracked after prolonged testing (>30 days). Analysis of the fracture area of the samples showed a significant decline in fibrillation at the crack with biodiesel compared to water and air aged samples, indicative of a less ductile failure for the biofuel. For its tests, the samples immersed in the aqueous solution with 10% IGEPAL showed cracking in less than 1 day (approximately 20 hours). The fracture area of the IGEPAL aged samples showed a complete absence of fibrillation, exhibiting a brittle failure typical of an exclusively ESC response. Based on this comparison, considering the time to failure and the failure mode displayed with this PE grade, the nature of biodiesel was considered to share a tendency for ESC with IGEPAL, albeit with less aggressiveness.

With similar aggressiveness witnessed for biodiesel in the differing manners of dilution tested and with limited supplies of biodiesel available, the remainder of testing in this study was done using the aqueous solution with 10% biodiesel. The ESC observations with biodiesel in petroleum diesel were notably concerning for tank fabrication making future studies recommended, but for the purposes of examining the mechanism of ESC with biodiesel, the approach with an aqueous solution was preferred; an orange pigmentation by biodiesel that was left in a PE sample, showing its preferred areas of absorption during aging, was much more distinct with the aqueous solution.

### 4.3.2. Monitored aging of immersed PE samples in biodiesel

Simultaneously conducted with the ultrasonic testing discussed in a later section of this work, gravimetric analysis was used to monitor the absorption rates and final uptake amounts between the different grades of PE. Figure 4.1 shows the percent weight gain for the four PE grades plotted against immersion time in the aqueous solution with 10% biodiesel. The data of 3-5 repeats were fitted through a logarithmic function for each curve shown. The measurement was soon halted after crack initiation was observed in each case and while three of the PE grades could have their results presented on the scale of hundreds of hours, absorption data for HD 6908.18 was given in the scale of hours to reflect its rapid failure in the presence of biodiesel. In all grades, the rate of absorption of biodiesel was highest during the initial stages as it contacts the fibrillated surface in the notch. The rate of biodiesel absorption is always highest during this period as it is preferentially absorbed at the region of highest stress. The eventual decline in the rate of biodiesel absorption seen for all samples was explained by Böhning et al. [26] who studied the sorption and desorption behavior of biodiesel in PE and suggested a thin surface film of biodiesel existed to reduce the effective concentration gradient. The curves indicate that all grades had not fully reached equilibrium before cracking; however, the trends shown suggest little further weight gains was expected.

The polymer grades that did not crack (all HD 8660.29 samples and half of the LA 080 samples) showed the highest percent mass gain upon reaching the limits of the test at 1000 hours of immersion. HD 8660.29 showed a mass gain of 4.17±0.15% after not cracking, while the uncracked LA 080 samples showed a slightly lower gain of 3.78±0.51%. The cracked samples witnessed lower mass gain than the uncracked samples with the highest being LA 080 (3.66±0.22%), followed by HD 6605.70 (2.62±0.23%) and HD 6908.19 (1.65±0.26%). The HD 6908.19 control samples showed no signs of cracking and a negligible weight gain in water (0.24%) at 7 hours. This grade will eventually fail in water due to SCG after approximately 17 hours of ageing.

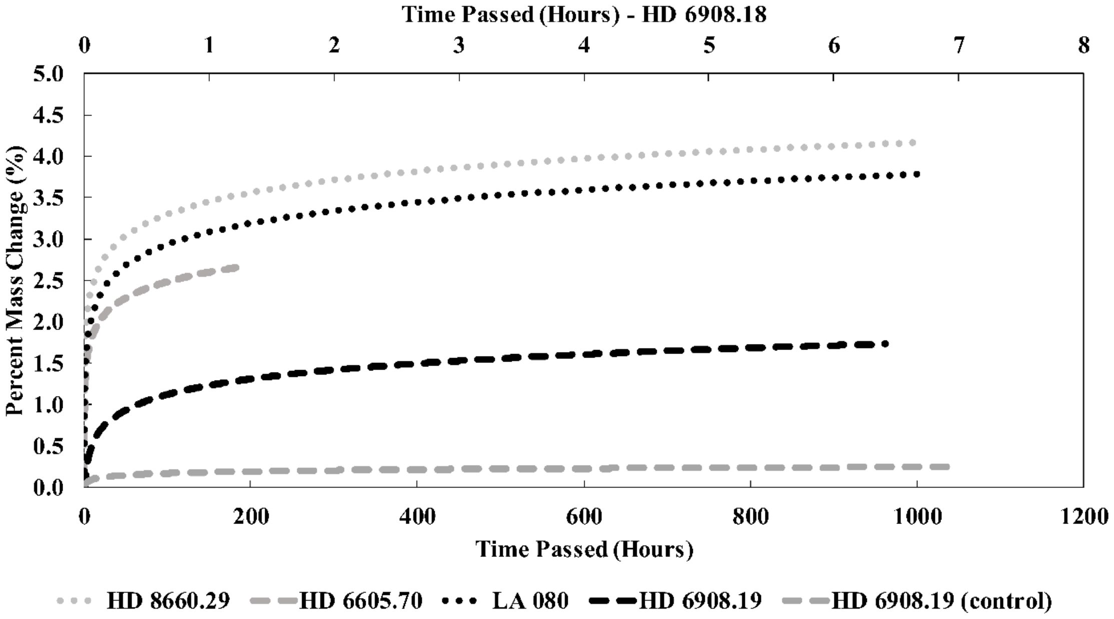

**Figure 4.1.** Plot of average percent weight change (%) vs. immersion time (hours) in 10% biodiesel for HD 8660.29 (gray dotted line), HD 6605.70 (dark gray dashed line), HD 6908.19 (black dashed line), and LA 080 samples (black dotted line). A control was run in water for HD 6908.19 (gray dashed line). Experimental data points were fitted with a logarithmic curve. The average $R^2$ value for all four grades is 0.92 depicting a good correlation. Results of polymer grade HD 6908.19 were plotted on a secondary x-axis due to the large difference in immersion time.

One of the reasons for the differing biodiesel absorption among the grades was their varying crystallinity. Measured at the notch by differential scanning calorimetry (DSC), the estimated crystallinity for each grade is shown in Table 4.2. The lower mass gain seen corresponded with the highest crystallinity associated, for example HD 6908.19 in comparison to HD 8660.29. The higher crystalline content (lower amorphous content) presents a more torturous path for the absorbed biodiesel to collect in the amorphous regions of the polymer resulting in a material with lower permeability to biodiesel [30].

**Table 4.2.** Summary of final mass change, ESCR ($F_{50}$ hours) in biodiesel, and the estimated crystallinity values by DSC.

| | **PE Grade** | **Crystallinity (%)** | **Mass Change (%)** | **ESCR ($\mathbf{F_{50} hours, biodiesel}$)** |
|---|---|---|---|---|
| **Uncracked Samples** | **HD 8660.29** | 50 | 4.17±0.15 | >1000 |
| | **LA 080 - Uncracked** | 61 | 3.78±0.51 | >1000 |
| **Cracked Samples** | **HD 6605.70** | 58 | 2.62±0.23 | 158.82±9.33 |
| | **LA 080 – Cracked** | 61 | 3.66±0.22 | 716.03±47.75 |
| | **HD 6908.19** | 69 | 1.65±0.26 | 4.73±0.40 |

The slight yellow-like color of biodiesel offered an interesting opportunity to visually track the preferred locations of absorption in the bent samples over time. PE grades that would crack exhibited a dark yellow color at the crack and some distance away from the crack, but the rest of the bar would only change to slight yellow color (if at all). Conversely, PE grades that did not crack would show a deeper yellow color all over the sample but never reach such a dark color. Visual inspection of the HD 8660.29 samples showed yellow staining over the whole body and not just at the notch. Conversely, darker yellow staining primarily at the crack was seen with HD 6605.70 and HD 6908.19 samples. The grade LA 080 represented a unique case. Approximately 50% of the time, immersed samples would fail and, in those cases, the coloration was localized but otherwise the whole body exhibited yellowing. This was a fascinating general observation since it highlighted early in the test that a sample was more likely to crack at some point if the notch region got darker in color.

Figure 4.2 shows the FT-IR spectra in the range of 1700-1800cm$^{-1}$ of microtomed cross-sections taken at the crack/notch area (Figures 4.2 (a) and 4.2 (c)) and at the opposite end of the rectangular sample (Figures 4.2 (b) and 4.2 (d)) for HD 6605.70 (failed) and HD 8660.29 (did not fail). The bottom spectrum in each plot corresponded to a blank (i.e. sample of the grade that was never immersed in solution), whereas the three spectra above corresponded to the absorbed biodiesel at the exposed surface of the samples and at 100-micron and 400-micron increments deeper. The characteristic peak showed in each spectrum at 1735-1750 cm$^{-1}$ corresponded to the ester of biodiesel, highest in intensity at the surface of samples to highlight greatest concentration while rapidly declining in intensity in the deeper cross-sections to indicate limited penetration. The results showed significant differences at a depth of 100 micron but minimal differences deeper (looking forward to the 400-micron depth spectra in the figure). Focusing on the cross-sections at 100-micron depth in all four plots, the opposite end of the samples had the lowest amount of biodiesel absorbed and was similar in concentration between the two grades examined (plots (b) and (d) in the figure). Conversely, the cross-sections at the notch showed a higher concentration of biodiesel (plots (a) and (c) in the figure), though markedly greater in the grade that cracked. These results seem to confirm the visual observations of more highly localized fluid absorption with ESC, though the FT-IR analysis notes that the higher surface area of the notch afforded greater biodiesel absorption even when the sample did not fail.

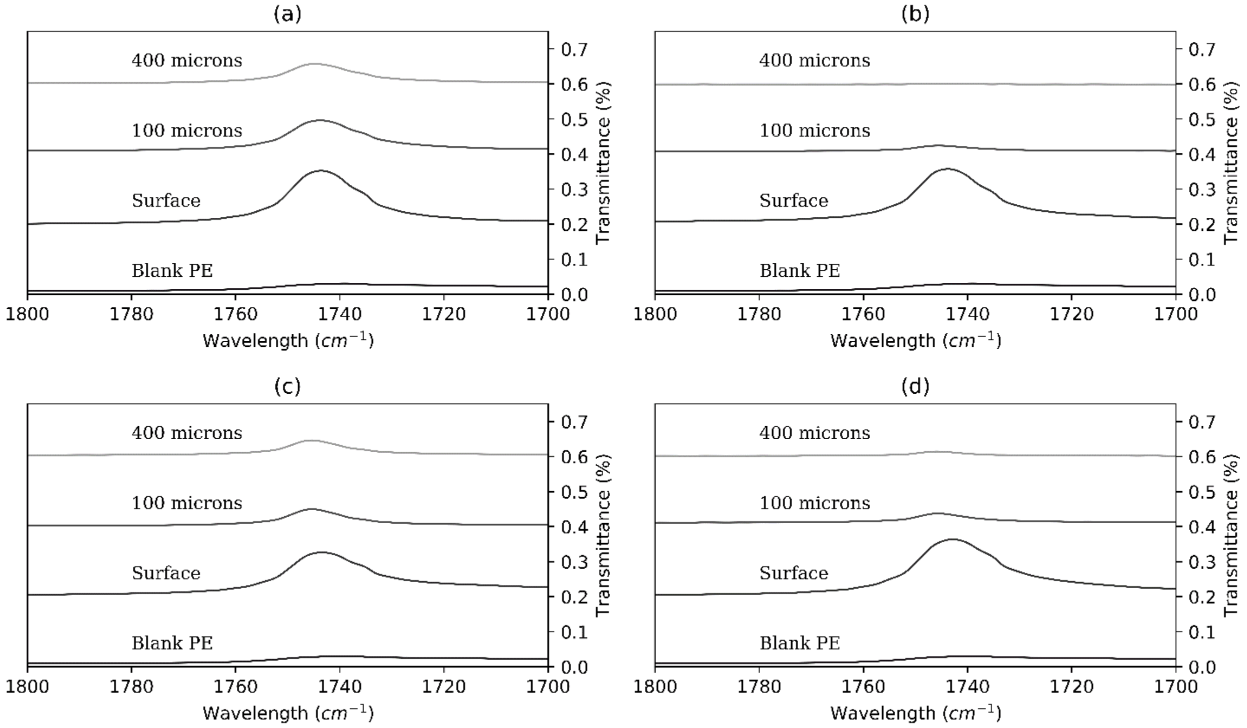

**Figure 4.2.** FT-IR (AT-R) spectra of **a)** (top left) HD 6605.70 – crack side; **b)** (top right) HD 6605.70 – side opposite to crack; **c)** (bottom left) HD 8660.29 – notch side; **d)** (bottom right) HD 8660.29 – side opposite to notch. To allow better visualization of the changes, results were restricted to the footprint peak of the ester functional group of biodiesel (1735-1750 $cm^{-1}$) and each spectra attained was displaced by 0.2 above the preceding spectra.

### 4.3.3. Analysis by nonlinear ultrasonics

Over the entire period of immersion in the modified Bell Test, penetration of biodiesel into a bent PE sample was monitored regularly using nonlinear ultrasonics for bulk assessment of internal stresses and identification of any modifications of the semi crystalline structure. The ultrasonic technique based on guided waves provided the ability to distinguish morphological changes pertaining to the inter-crystalline region of the polymer without destructive testing such that a sample could be returned to the Bell Test for further aging. Earlier investigations with this ultrasonic technique showed a decrease in the “ultrasonic attenuation ratio” (increase in signal attenuation) related to an increase in relaxed stresses, in both time and frequency domain, from plastic deformation. The change in ultrasonic signal was done in recognition to PE’s dispersive nature of the ultrasonic waves and defined as the amplitude after deformation over the undeformed sample maximum amplitude peak [33]. The revised technique used in the present paper [31], on the other hand, is based on the changes in the amplitude of the third harmonic region, which was chosen with recognition of the third harmonic peak being the most important and strongest frequency in planar waves to represent the changes in the semi crystalline structure of PE with increased reliability in terms of signal-to-noise ratio. The primary assumption of this ultrasonic technique is that propagation of ultrasonic waves in PE will be dispersive and different from a perfect elastic body. Thus, the non-linear interaction of the ultrasonic vibrations with the discontinuities of a semi-crystalline network (such as those created by the penetration of solvents) will generate frequencies different from original wave introduced, which are detectable in the higher order harmonics [31, 34, 35]. Results using the latter method [30] have shown an increase in the amplitude of the third harmonic region related to the increasing internal stresses from plastic deformation and chemical swelling.

Figure 4.3 shows two examples of the spectral pattern pertaining to HD 6605.70, before immersion and after cracking in the aqueous solution with 10% biodiesel, with denoted changes in the distinct third harmonic region ($A_3$, between 400-500 kHz) being highlighted. Second order and other higher order harmonic peaks were attenuated in the dispersive material and thus not used for analysis. The amplitude ratio (ultrasonic parameter) based on the third harmonic peak ($A_3$) relative to the input peak ($A_1$), is used as a descriptor to quantify the changes in the generated third harmonic region. The change in the ultrasonic parameter occurs in response to changing internal stresses due to microstructural asymmetries and discontinuities created by penetrating molecules [36]. A previous investigation [30] on plasticization properties of biodiesel and toluene used this ultrasonics method to identify the different modes of interaction between the two fluids with the semi-crystalline structure of PE. Being plasticized by toluene produces an increase in the ultrasonic parameter (amplitude of third harmonic peak) which occurred in response to the increasing internal stresses created by the penetrating molecules. On the contrary, penetration by biodiesel produces a decrease in the ultrasonic parameter in response to a relative decrease in internal stresses, explained as promoted crystal slip during plastic deformation. Those findings were consistent with the observations of the fracture areas of the biodiesel aged samples mentioned earlier in this study. The samples aged in biodiesel exhibited a significant decline in fibrillation at the crack in comparison to water- or air-aged samples. ESC is a physical phenomenon, meaning that the biodiesel in contact with the stressed polymer does not chemically alter the polymer structure, but embrittles it due to the physical interaction of the environment with the polymer chains [37]. From a macroscopic perspective, the brittle fracture appears as a clean break with a characteristic smooth surface with minimal fibril generation. The brittle failure evident in the biodiesel-aged samples corresponded to the assisted disentanglement of the interlamellar linkages that promoted crystal slip in the stressed polymer by the presence of an active environment, such as biodiesel. The promoted crystal slip decreased the internal stresses within the polymer, which resulted in the decreased third harmonic peak ($A_3$) in Figure 4.3.

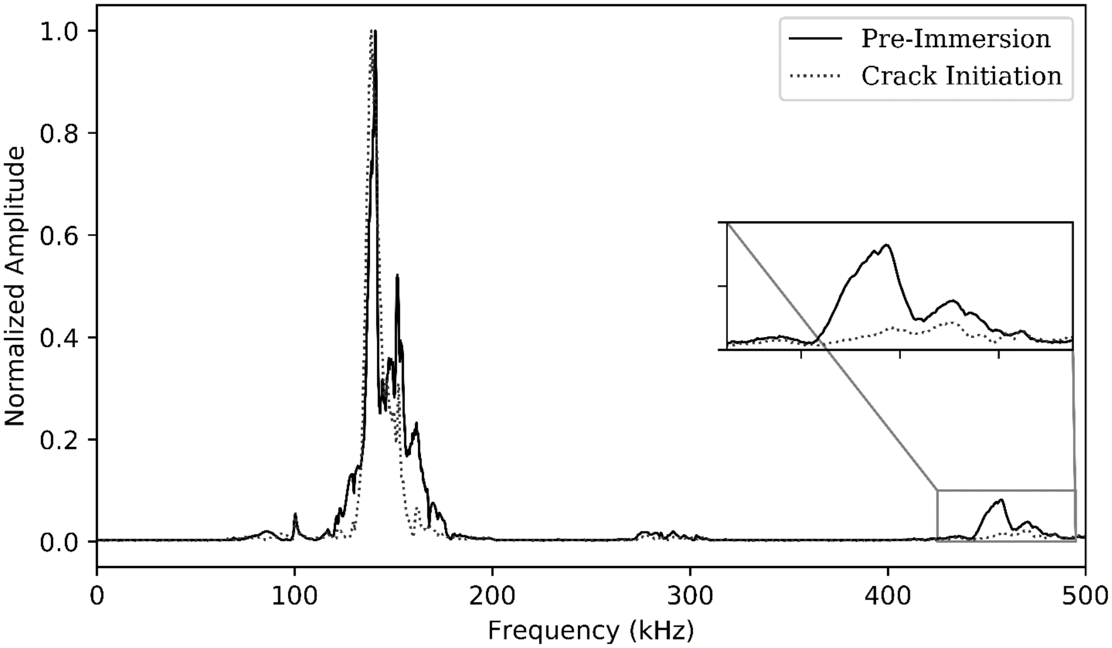

**Figure 4.3.** Ultrasonic spectra for the HD 6605.70 sample before testing and after cracking due to biodiesel immersion. The region highlighted in the box corresponds to the third harmonic region ($A_3$, between 400-500 kHz).

Figure 4.4 plots the percent change in the nonlinear ultrasonic parameter ($A_3/A_1$) for HD 6605.70 and HD 6908.19, which showed localized yellowing at the notch of their bent samples while immersed in the aqueous solution of 10% biodiesel. Since both grades exhibited failures in the presence of biodiesel, the point when crack initiation began was marked in the plots for reference; a micrograph of the type of cracking observed is included in the figure for HD 6605.70. Three samples for each grade are shown to highlight the trend being observed by the acoustic technique, presented on the basis of mass absorbed (Figures 4.4 (b) and 4.4 (d)) and immersion time (Figures 4.4 (a) and 4.4 (c)); on a time basis the trend was similar between different grades but it differed significantly on a mass basis. On the basis of immersion time, there was always a significant decrease in the ultrasonic parameter that can be related to decreases in internal stresses [30]. The rate of absorbed biodiesel was always highest during this period as it contacted the fibrillated surface inside the notch (as noted in Sec. 3.2). This localized absorption of the fluid at the notch, by what is presumed to be stress-enhanced diffusion, plasticizes the polymer reducing the load-bearing resistance of the inter-crystalline chains in the amorphous regions and causing a decrease in the ultrasonic parameter to a minimum value. This minimum ultrasonic parameter is referred herein as the "critical ultrasonic parameter value". A plateau is seen at this minimum value for a considerable period of time before the parameter increases ahead of crack initiation, as seen on Figures 4.4 (a) and (c) for both polymers. The biodiesel is believed to relieve the accumulating stresses due to deformation of the sample until just before cracking. Once cracking began, the parameter value decreased again but since the propagation path for the ultrasonic wave was no longer intact at this point, the change cannot be interpreted as directly related to the morphology of these polymers.

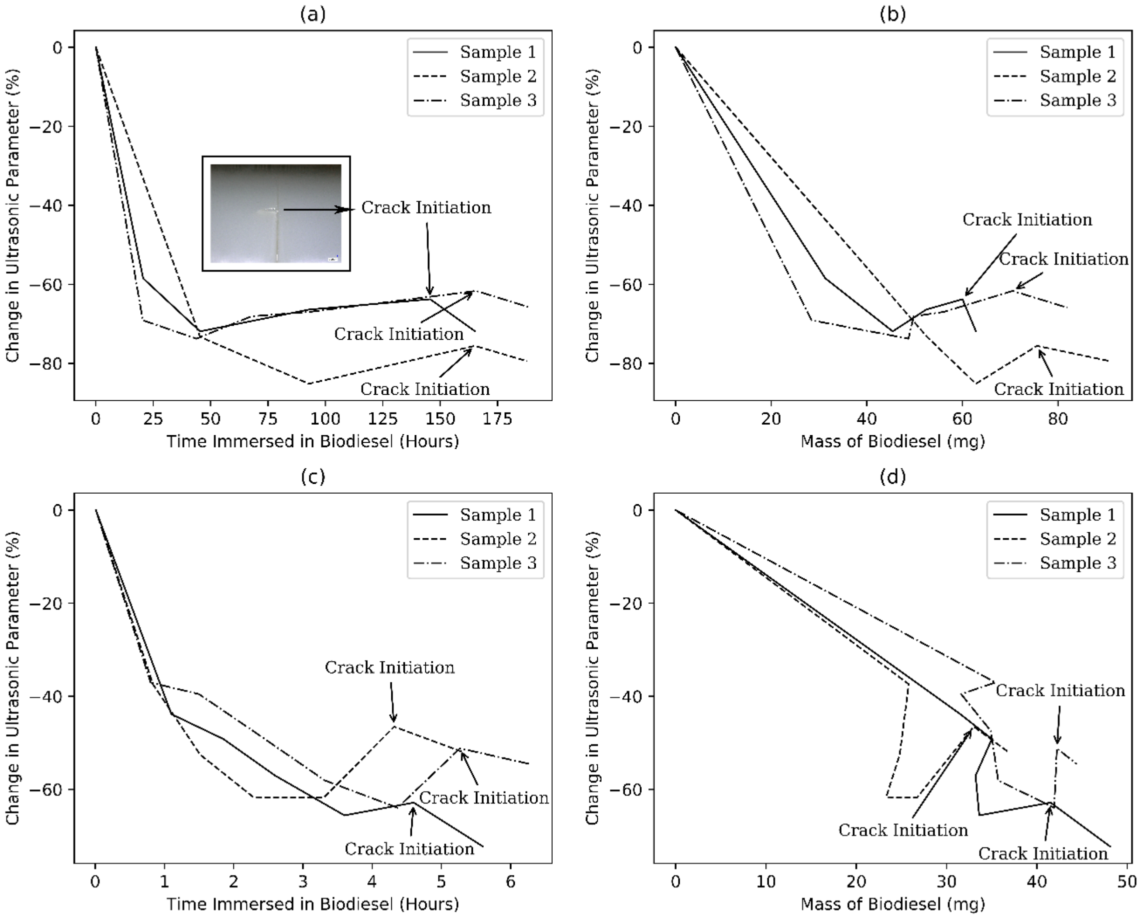

**Figure 4.4.** Variation in nonlinear ultrasonic parameter (%) vs **(a)** (top left) time immersed in biodiesel (Hours) for three HD 6605.70 samples; **(b)** (top right) mass of biodiesel absorbed (mg) for three HD 6605.70 samples; **(c)** (bottom left) time immersed in biodiesel (Hours) for three HD 6908.19; **(d)** (bottom right) mass of biodiesel absorbed (mg) for three HD 6908.19 samples. Time at which cracking was first visually observed for each sample has been labelled as "crack initiation" on the plot and microscopic imaging of crack initiation of Sample 1 of HD 6605.70 has been added.

As a matter of comparison, Figure 4.5 plots the percent change in the ultrasonic parameter ($A_3/A_1$) for a control, in this case HD 6908.19 immersed in water. The three samples in the control appear similar to each other in trend relative to immersion time. The initial decrease in the ultrasonic parameter occurred in response to decreasing internal stresses due to relaxation of the sample after notching and bending. Test methods, such as the Bell Test, where deformation occurs under constant strains are known to be less severe than tests deforming at constant stress (Ex. The PENT test), since stresses are allowed to relax in the former case [2]. The following increase in the ultrasonic parameter occurred in response to increasing internal stresses related to the SCG behavior mentioned above. The decrease in the ultrasonic parameter that follows cracking cannot be attributed to material features since the specimen dimensions have now been radically changed, which will affect propagation of the acoustic wave.

Physical properties of semi-crystalline polymers are believed to be governed primarily by the presence of intra-crystalline molecular connections in the amorphous regions that hold crystallites in proximity to one another together, such as cilia (chain ends protruding from crystallites), loose loops (chains that begin and end in the same lamella), and tie molecules (TMs) (high molecular weight polymer chains that begin and end in adjacent crystalline lamella). The latter has been recognized as being the most important crystalline/amorphous interaction due to its influence on short-term properties, such as stiffness and strength, as well as long-term properties of semi-crystalline polymers [38, 39]. Loose loops or cilia in the amorphous regions entangle to give rise to a weaker interaction that helps hold the crystalline structure together [39]. For the sake of uncomplicatedness, all further explanations regarding these crystalline/amorphous interactions will be primarily based on TMs. The application of a load normal to the face of a crystalline lamellae in the bent samples causes these TMs to stretch; and after some time the long-term low-level stress causes the TMs to extend and ultimately fail until their numbers are insufficient to withstand the load applied; slippage or breakage of adjacent lamella occurs, which generates a void; and consequently, crazing begins which ultimately leads to the slow crack growth behavior [38].

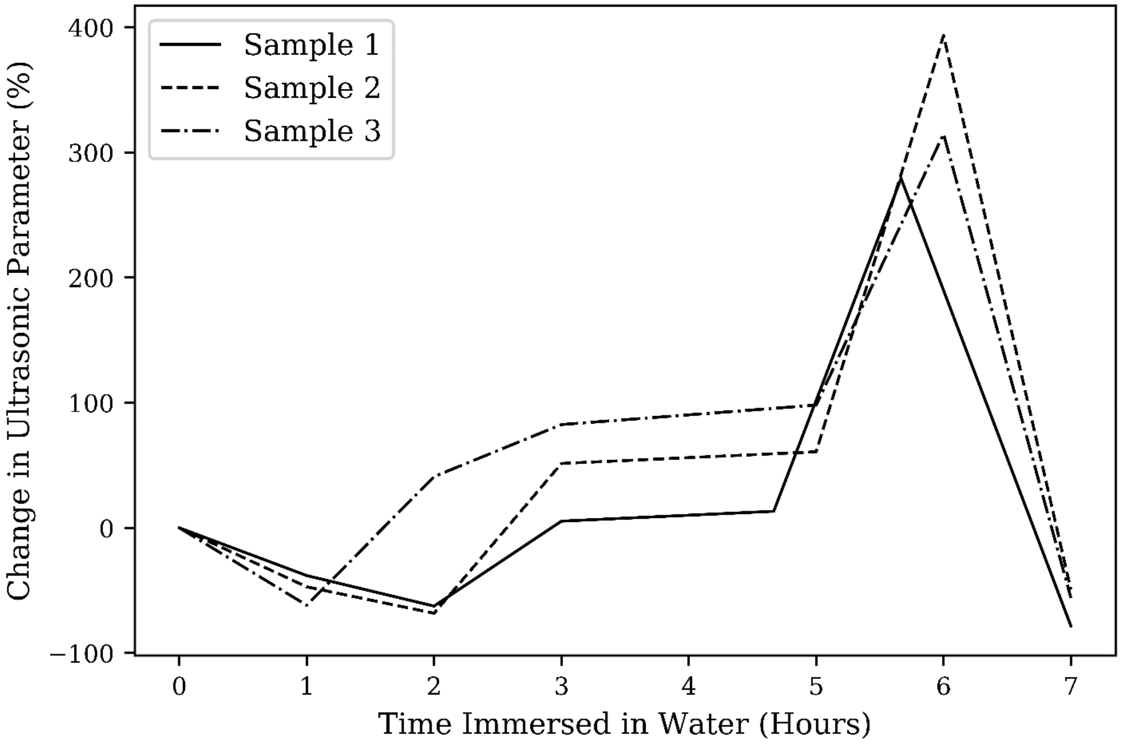

**Figure 4.5**. Variation in nonlinear ultrasonic parameter (%) vs time immersed in water (Hours) for three HD 6908.19 samples.

The results in Figures 4.4 and 4.5 are hypothetically following the localized stresses in the interlamellar region caused by the penetration of biodiesel. As mentioned above, the decrease in the ultrasonic parameter to the minimum value (critical ultrasonic parameter) is a result of the plasticization of the tie chains from localized fluid absorption at the notch. The critical ultrasonic parameter is seen as a critical element of the ESC mechanism. At this stage, the nature of the stresses related to SCG appeared momentarily in balance with the influences of plasticization that represent the two opposing natures determining the effect of biodiesel on a grade of PE.

Conversely, in cases where the fluid had a great affinity for the whole plastic body, without localized absorption of the fluid (ref to Sec. 3.2), the polymer generally did not demonstrate ESC, which for the acoustic analysis was highlighted with HD 8660.29. LA 080 was included in this section since it sometimes did not crack but also because its coloration shifted depending on whether it would crack or not. Figure 4.6 (a-d) shows the percent change in the nonlinear ultrasonic parameter for HD 8660.29 and LA 080 on both a time basis and mass gain basis while immersed in the aqueous solution of 10% biodiesel. The included micrograph shows only a notch without cracking after >1000 hours of immersion. On the basis of time, the plots appear similar though for the majority of tested samples that did not crack, there was no rise in the acoustic parameter after reaching the critical value. The case of LA 080 looks closer to HD 6605.70 and HD 6908.19, on the basis of time, shown in Figure 4.6 (c). The percent change in the acoustic parameter declined well below -60 for all three grades whereas for HD 8660.29 it never dropped below -50. The two shown cases of cracked samples

(Samples 1 and 2) for LA 080 showed a trend in the parameter like described for HD 6605.70 and HD 6908.19 with the rise in value prior to cracking and likewise, showed similar trends for the two samples that did not crack (Samples 3 and 4) to HD 8660.29.

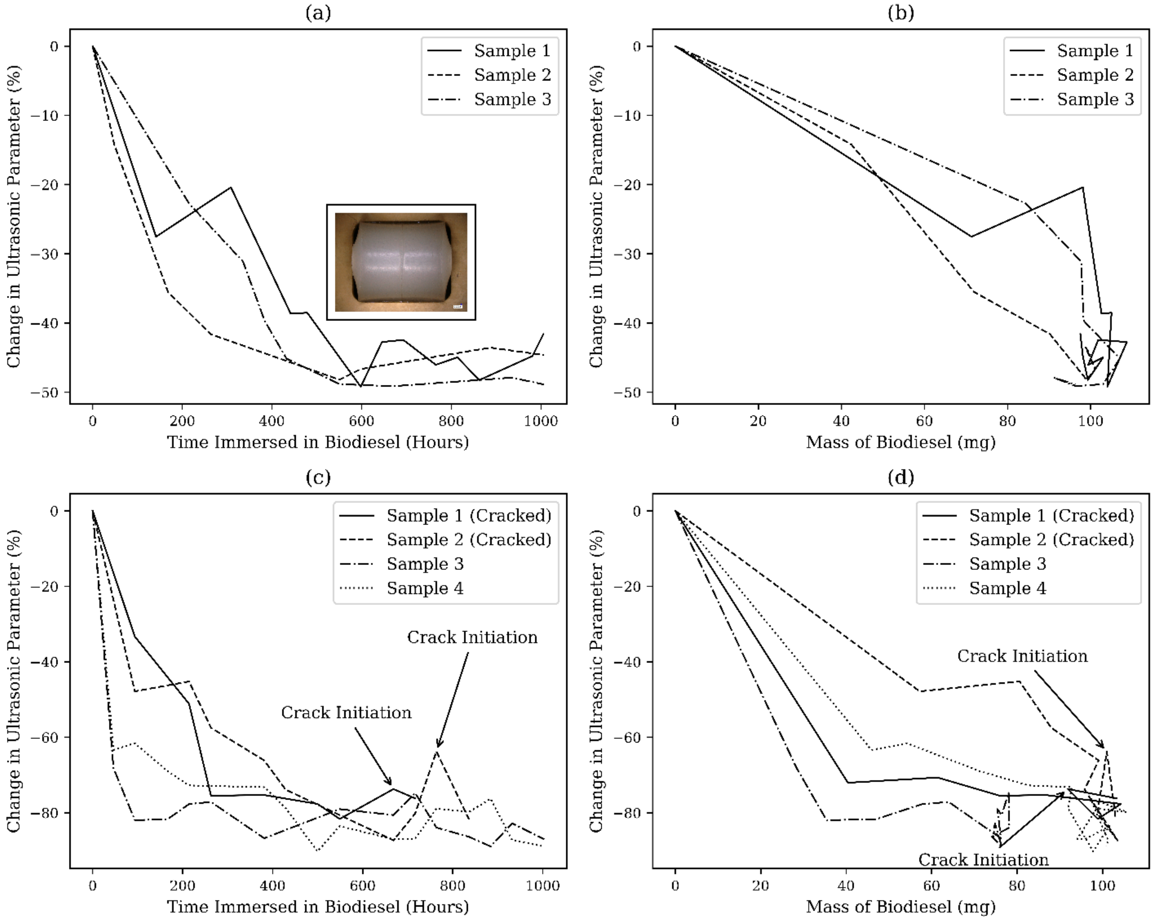

**Figure 4.6.** Variation in nonlinear ultrasonic parameter (%) vs **(a)** (top left) time immersed in biodiesel (Hours) for three HD 8660.29 samples; **(b)** (top right) mass of biodiesel absorbed (mg) for three HD 8660.29 samples; **(c)** (bottom left) time immersed in biodiesel (Hours) for four LA 080 samples; **(d)** (bottom right) mass of biodiesel absorbed (mg) for four LA 080 samples. Time at which cracking was first visually observed for each sample that cracked has been labelled as "crack initiation" on the plot. Microscopic imaging of the notched area of Sample 1 of HD 8660.29 after >1000 hours of immersion in biodiesel has been added to the plot.

The analysis on a mass basis did not produce a consistent identifiable trend (Figure 4.5 (b, d) and Figure 4.6 (b, d)) between the different PE grades, even though gravimetric, visual and FTIR results point to a relationship between ESC and absorbed fluid. The time and mass basis trends for LA 080 and HD 6605.70 were similar, presumably showing that the failure was driven by both factors simultaneously and would be consistent with the expected mechanism for ESC. However, the mass basis trend for HD 6908.19 that failed, looked more closely like the observed trend with HD 8660.29 (did not fail). This may be a valuable insight since HD 6908.19 has the shortest failure time of the tested grades and this analysis could be interpreted as determining the grade did not fail by ESC but rather SCG. The reported failure time in water, seen in Figure 4.5, at approximately 7 hours is quite close to the ESCR time with biodiesel, so the explanation is plausible. Conversely, this grade absorbed the least amount of biodiesel in our tests and it is also possible that the plate waves of the acoustic method lack the resolution to properly detect the localized phenomena. More studies of polymers with very short ESCR values would be appropriate to address this interesting outcome.

### 4.3.4. Proposed mechanism for environmental stress cracking by biodiesel on PE

The basis of the proposed mechanism in this work was founded on the hypothesis that the concentration-limited plasticization mechanism proposed by Rogers et al. [10] for environmental stress cracking explained the nature of biodiesel with polyethylene (PE). The following outlines key elements of their plasticization mechanism as it applied to biodiesel in the Bell Test, using Figure 4.7 as an aid in the explanation:

1. Fibrillation is initiated at the notch tip of bent specimens as shown in Figure 4.7(a). Stresses are concentrated at the front of the notch, as shown by Step 1 of Figure 4.7(b).
2. Biodiesel contacts the increased surface area of fibrillated mass inside the notch, being preferentially absorbed at this site of higher stresses. Studies by Hittmair and Ullman [40] have shown increased penetration of liquids into polymers experiencing increased stresses. If the contacting fluid has a plasticizing nature on the polymer, like biodiesel with polyethylene, then the localized absorption is a means to lower the energy in the material. For environmental stress cracking, the polymer experiences reduced inter-lamella strength by plasticization of the tie chains in the amorphous regions of the fibrils (Step 2).
3. A critical component of Roger's mechanism is the limited effectiveness of the stress cracking agent as a plasticizer so that its effects are constrained to the amorphous regions but not upon the crystals. The diffusion rate should decline in the highly oriented regions making up these fibrils yet this behavior seems to be countered by driving forces to lower the local energy state where stresses have become concentrated. Therefore, stress-enhanced diffusion takes place at the ends (shoulders) of the fibrils. The shoulders have the most disrupted morphological structure, which helps diffusion and sorption.
4. The tie chains, still experiencing distorting stresses in the notch despite plasticization, begin to fail and crazing is initiated as a result (Step 3).
5. Microscopic voids in the formed crazes coalesce and initiate a smooth crack with

very little fibril generation, which extends beyond the original localized stress region of the notch. A new localized high stress region is formed at the crack tip and Step 2 is repeated again (Step 4). Lustiger et al. [41] have shown evidence of the formation of secondary crazes in samples undergoing environmental stress cracking.

6. The crack continues to grow progressively, in the same manner, over a thin plane normal to the applied stress, resulting in failure of the material (Steps 5 and 6).

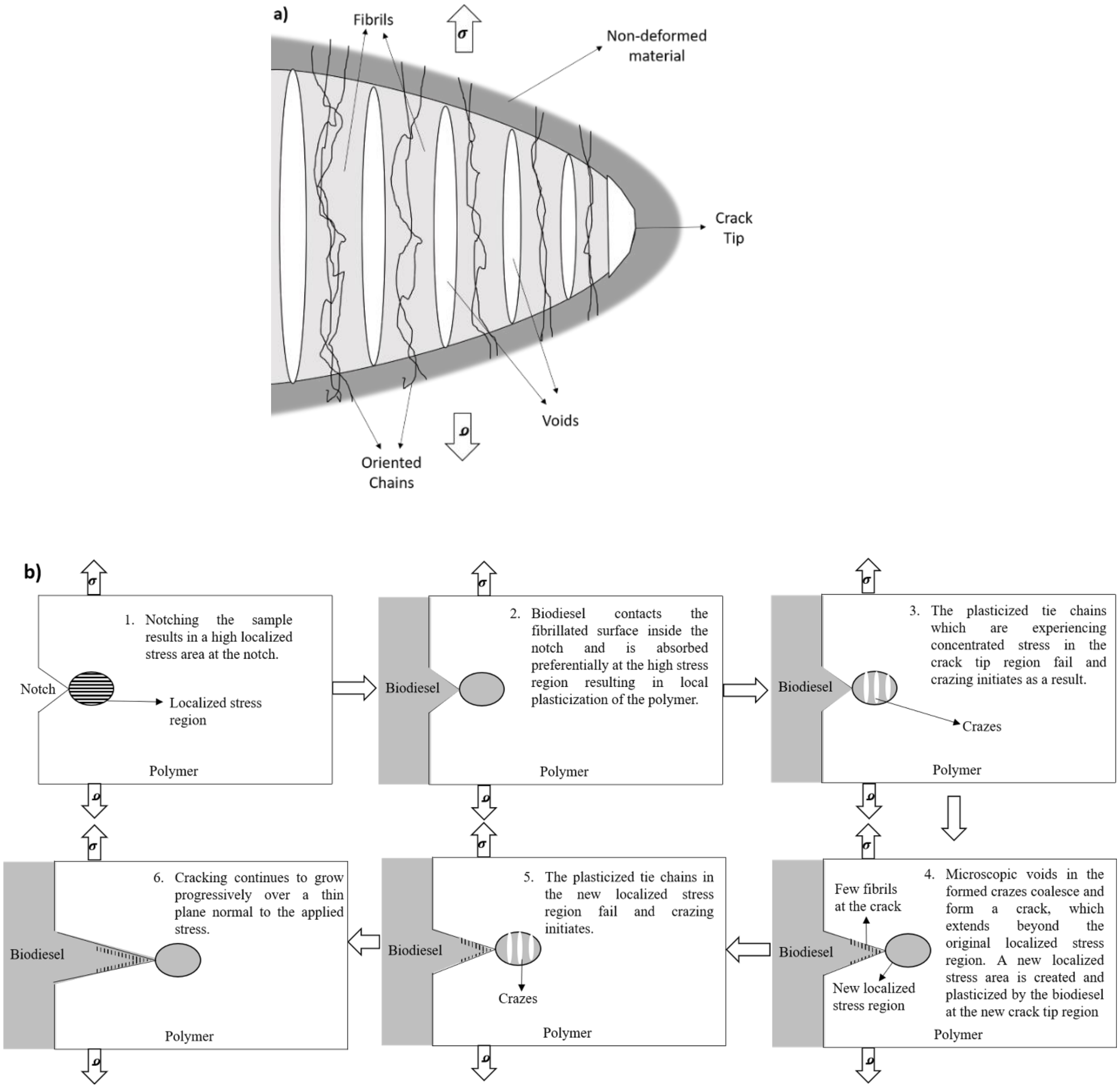

1. Notching the sample results in a high localized stress area at the notch.
2. Biodiesel contacts the fibrillated surface inside the notch and is absorbed preferentially at the high stress region resulting in local plasticization of the polymer.
3. The plasticized tie chains which are experiencing concentrated stress in the crack tip region fail and crazing initiates as a result.
4. Microscopic voids in the formed crazes coalesce and form a crack, which extends beyond the original localized stress region. A new localized stress area is created and plasticized by the biodiesel at the new crack tip region
5. The plasticized tie chains in the new localized stress region fail and crazing initiates.
6. Cracking continues to grow progressively over a thin plane normal to the applied stress.

**Figure 4.7.** Conceptual drawing of environmental stress cracking. **(a)** Fibrillated fracture occurring at the crack tip; **(b)** mechanism of environmental stress cracking of polyethylene by biodiesel.

Experimental results from this investigation suggest that the mechanism presented is the most probable pathway for ESC of PE by biodiesel in the Bell Test. In the early stages of immersion, surface absorption of biodiesel is rapid across the whole specimen, but the fibrils generated at the notch tip provide an increased surface area for the preferential absorption of biodiesel at the site of higher stresses. The deforming stresses can enhance sorption and diffusion in the local region in the presence of the fuel reducing the density of the amorphous phase [42]. Results from FT-IR (Figure 4.2) and visual inspection of the failed samples have shown higher concentrations of biodiesel at the notch/crack area depicting this localized absorption behavior. The concentrated plasticization effect of biodiesel at the notch decreased the ultrasonic parameter in response to lowered internal stresses created by the penetrating molecules (Figure 4.4 (a-d)). We note from our findings that polymers which will never crack by ESC but are influenced by the fluid, are unlikely to show this specific localized absorption.

The critical element of the entire ESC mechanism is thought to be Phase 3. At this stage, the ultrasonic parameter is at its minimum value (critical ultrasonic parameter) and two opposing phenomena (internal stresses concentrating in the tie molecules at the notch versus relief of those stresses through plasticization by the penetrating biodiesel) appear on the bulk to be momentarily in equilibrium. Two outcomes present themselves after this point: (i) no failure (middle ground response where plasticization negated the buildup of stresses), or (ii) brittle failure; the other extreme not stated above will be when a stress-induced ductile failure results with no influence by the contacting fluid but this case does not fall under the ESC mechanism (for example, Figure 4.5 for HD 6908.19 in water). The unique case of LA 080 offers the opportunity of analyzing these two outcomes for ESC by biodiesel. For the samples of LA 080 that cracked, the ultrasonic parameter increased eventually after being for some time at the critical value indicating that localized stresses had overcame the plasticization effect by biodiesel, just as seen with HD 6605.70. It is telling that ESC never occurred during the period of rapid fuel absorption by the PE samples, but rather once the rate of mass gain had slowed, and that failure times were shorter with less mass gained (Sec 3.2). The high anisotropy of diffusion and the significant reduction of sorption and diffusion occurring gradually over time (witnessed in the mass gain curves) are attributed to the microfibrillar morphology of PE that is becoming increasing aligned due to the bending stresses. The closely packed taut/stretched TMs reduce many sorption sites and decrease diffusivity locally [42]; Peterlin [43] has likened the taut TMs to crystals reducing the internal channels for a penetrant. The acoustic parameter rose in value at this point in the mechanism, responding to increasing internal stresses and signaling imminent failure of the sample; for the sake of explaining the mechanism, it seems the equilibrium corresponding to the critical acoustic parameter is eventually lost as less biodiesel enters to plasticize the building internal stresses.

Figure 4.5 showed that internal stresses increase over time in the bent specimens, though the failure time in this case was now much longer without an ESC agent. The source of building internal stresses seen by acoustics, and being a critical pervasive component of the ESC mechanism, comes from ‘weak points’ between different regions caused by the non-uniform plastic deformation of a bent sample [44]. These ‘weak points’ can be generated chemically, thermally, and mechanically by non-uniform plastic deformation and by crack generation [45, 46].

Reflecting on IGEPAL which experiences lower absorption in PE (~0.25 wt%, found in a parallel study by the authors) and earlier failures (Table 1) than biodiesel, we see a minute amount of plasticization accelerates ESC (affecting the TMs without overall relief of building internal stresses), more plasticization slows ESC (affecting the TMs but also relieving overall stresses while sufficient agent is being progressively absorbed), and too much plasticization where internal stresses are being relaxed permanently and no cracking results (HD 8660.29 and some samples of LA 080).

The whole-body coloration seen by the non-cracking samples is explained by the profound penetration of the fuel that resulted in the higher mass gains (4.17 wt% in HD 8660.29 and 3.78 wt% in uncracked LA 080) reflected in the mass gain plots (Figure 4.1). The high absorption of biodiesel in PE halted ESC through excessive plasticization resulting in equilibrium of the critical ultrasonic parameter (Figure 4.6). On the contrary, the loss of this equilibrium in the critical ultrasonic parameter is justified by the localized coloration and reduced whole body coloration seen by the cracking samples. The localized coloration is interpreted by the localized absorption and consequently higher concentrations of biodiesel at the notch (Figure 4.2). The reduced whole-body coloration in the cracked samples is explained by the slowed down absorption of biodiesel that eventuated in the lower mass gains (1.65 wt% HD 6908.19, 2.62 wt% in HD 6605.70, and 3.66 wt% in crack LA 080) reflected in Figure 4.1. The decreased absorption in PE reduced the amount of plasticization resulting in loss of equilibrium of the critical ultrasonic parameter (Figure 4.4). The increasing internal stresses in the bent specimens increased the ultrasonic parameter until the stress-induced failure occurs. The lower failure times in the cracked PE grades with lower biodiesel weight gain (Table 2) is seen as darker localized coloration at the crack reflecting the effect of concentrated plasticization by biodiesel localized at the notch on acceleration of ESC.

It seems probable that the samples that did not crack in biodiesel have a different arrangement of the tie chains in the interlamellar region than those that cracked which caused the bulk plasticization effect of biodiesel to negate the localized stresses at the notch and prevent crack growth in the samples. LA 080 must exist at the boundaries of molecular structure and crystallization kinetics to obtain a density of tie chain sensitive enough to minor variations in solidification that gives both possible outcomes.

### 4.3.5. Interaction of biodiesel with the different grades of polyethylene

This last section considers the differences and similarities in the ESCR results presented in Table 4.1 for the standard IGEPAL detergent versus Table 4.2 with biodiesel, based on the grades of PE. The findings attained in this investigation show consistency between the two ESC media based on the trend in $F_{50}$ failure times relative to the different grades, with a potential correlation between the crystalline content and the molecular weight of the polymer (crudely implied in this case by MFI). Apart from LA 080, an inverse correlation is seen between the crystalline content of the samples and their ESCR by biodiesel. Polymer grade HD 6908.19 with the highest crystalline content (69%) and lowest molecular weight (highest MFI - 8.2 g/10 min) showed the lowest resistance to ESC by failing quicker than all the other grades after 4.73±0.40 hours by biodiesel and 3 hours with IGEPAL. The low molecular weight associated with the polymer decreased the probable formation of TMs and the high crystallinity increases the stiffness of the sample, which induced large stresses on fibrils in the notch when bent. We did note earlier that this grade might not be failing by ESC, with cracking unrelated to the environmental fluid, but since its failure time in biodiesel was greater than in water it was still considered an ESC failure in this discussion. The grade with the second lowest resistance to ESC was HD 6605.70 at 158.82±9.33 hours (20 hours with IGEPAL). Its relatively high crystallinity (58%) and low molecular weight (high MFI – 5.0 g/10 min) have made it susceptible to ESC by biodiesel but with a higher resistance than HD 6908.19. The higher molecular weight and lower crystallinity of this grade in comparison to HD 6908.19 have allowed it to last longer in biodiesel without cracking.

The grade HD 8660.29 showed the highest resistance to ESC by biodiesel by not cracking despite being immersed for >1000 hours (40 hours with IGEPAL), by having the lowest crystallinity (50%) and a relatively higher molecular weight (low MFI – 2.0 g/10 min) to the others tested. Our previous investigations [30] on this polymer grade showed great fuel uptake and consequently a greater extent of plasticization by biodiesel with this low crystallinity/low density grade due to its large free volume ($V_f$) on account of the greater amorphous content.

The correlation between resistance to ESC by biodiesel and crystallinity that was seen in the other polymers could not be seen with LA 080 and this can be attributed to its very high molecular weight (very low MFI – 0.3 g/10 min). LA 080 was found to be susceptible to both ESC and plasticization by biodiesel. The samples that cracked in biodiesel failed after 716.03±47.75 hours (47 hours with IGEPAL). It seems that the high crystallinity (61%) of this PE grade has made some samples susceptible to ESC; while the very high molecular weight and low density (0.934 g/cm$^3$) have made some samples of this grade resistant to ESC and prone to plasticization by biodiesel instead.

## 4.4. Conclusions

The investigation into the compatibility of biodiesel with PE for use in fuel-contact services has revealed that the biofuel possesses both ESC and plasticization properties towards the polymer. The fatty acid methyl ester was found to be a plasticizing agent for all grades of PE but more of an ESC agent to some, with the different modes of interaction attributed to the crystalline content and molecular weight of the polymer.

The different effects of biodiesel were analyzed by following the localized stresses in the interlamellar region through the response of an acoustic signature generated from a novel non-destructive testing method based on ultrasonics. Simultaneous to ultrasonic testing, gravimetric analysis, infrared spectroscopy (FT-IR), and visual inspection of the biodiesel aged samples were used to propose a concentrated-limited plasticization mechanism for ESC of biodiesel with PE in the Bell Test. PE grades that would crack in biodiesel exhibited a dark yellow color at the crack and some distance away from the crack but the rest of the bar would only change to a slight yellow color (if at all). Conversely, PE grades that would not crack showed a deeper yellow color all over the sample but never reached the same darkness at the notch. These results, confirmed by FT-IR analysis, showed that a polymer which will never crack by ESC, will not show localized absorption of the ESC agent.

Furthermore, the findings attained in this investigation showed consistency between biodiesel and IGEPAL, a known ESC agent. Considering the time to failure and the failure mode displayed with PE, the nature of biodiesel was considered to share a tendency for ESC with IGEPAL, albeit with less aggressiveness. A potential correlation is seen between the crystalline content and molecular weight of the polymer and the failure times in both mediums. PE grades with higher crystallinity and lower molecular weights showed lower resistance to ESC by failing quicker.

Further investigations by our group will focus on attaining a deeper understanding of the conditions that promote the actions of biodiesel as an ESC agent and as a plasticizing agent.

## Acknowledgements

The authors would like to thank Imperial Oil Ltd. and the Natural Sciences and Engineering Research Council (NSERC) for funding the work. The authors would like to especially thank Ron Cooke at Imperial Oil for his advice, supply of materials, and technical insights, and Heera Maraway at the McMaster Manufacturing Research Institute (MMRI) and Vladimir Gritschine at McMaster University for their help with testing.

## References

[1] O.-G. Piringer, A.L. Baner, Plastic packaging: interactions with food and pharmaceuticals, Wiley-VCH, Weinheim, 2008.

[2] J.M. Lagarón, J.M. Pastor, B.J. Kip, Role of an active environment of use in an environmental stress crack resistance (ESCR) test in stretched polyethylene: Polymer. 40 (1999) 1629–1636. doi:10.1016/s0032-3861(98)00406-6.

[3] N. Pons, A. Bergeret, J.-C. Benezet, L. Ferry, F. Fesquet, An Environmental Stress Cracking (ESC) test to study the ageing of biopolymers and biocomposites, Polymer Testing. 30 (2011) 310–317. doi:10.1016/j.polymertesting.2010.11.015.

[4] A. Ward, X. Lu, Y. Huang, N. Brown, The mechanism of slow crack growth in polyethylene by an environmental stress cracking agent, Polymer. 32 (1991) 2172–2178. doi:10.1016/0032-3861(91)90043-i.

[5] J.J. Cheng, M.A. Polak, A. Penlidis, Influence of micromolecular structure on environmental stress cracking resistance of high density polyethylene, Tunnelling and Underground Space Technology. 26 (2011) 582–593. doi:10.1016/j.tust.2011.02.003.

[6] A. Ghanbari-Siahkali, P. Kingshott, D.W. Breiby, L. Arleth, C.K. Kjellander, K. Almdal, Investigating the role of anionic surfactant and polymer morphology on the environmental stress cracking (ESC) of high-density polyethylene, Polymer Degradation and Stability. 89 (2005) 442–453. doi:10.1016/j.polymdegradstab.2005.01.023.

[7] D.C. Wright, Environmental stress cracking of plastics, Rapra Technology, Shrewsbury, 1996.

[8] Arnold, J. C. "Environmental stress crack initiation in glassy polymers." *Trends in polymer*

*science* 4.12 (1996): 403-408.

[9] R.A. Isaksen, S. Newman, R.J. Clark, Mechanism of environmental stress cracking in linear polyethylene, Journal of Applied Polymer Science. 7 (1963) 515–531. doi:10.1002/app.1963.070070210.

[10] K. Tonyali, C.E. Rogers, H.R. Brown, Stress-cracking of polyethylene in organic liquids, Polymer. 28 (1987) 1472–1477. doi:10.1016/0032-3861(87)90344-2.

[11] M. Schilling, M. Böhning, H. Oehler, I. Alig, U. Niebergall, Environmental stress cracking of polyethylene high density (PE-HD) induced by liquid media - Validation and verification of the full-notch creep test (FNCT), Materialwissenschaft Und Werkstofftechnik. 48 (2017) 846–854. doi:10.1002/mawe.201700065.

[12] M. Schilling, U. Niebergall, I. Alig, H. Oehler, D. Lellinger, D. Meinel, et al., Crack propagation in PE-HD induced by environmental stress cracking (ESC) analyzed by several imaging techniques, Polymer Testing. 70 (2018) 544–555. doi:10.1016/j.polymertesting.2018.08.014.

[13] P. Sardashti, A.J. Scott, C. Tzoganakis, M.A. Polak, A. Penlidis, Effect of Temperature on Environmental Stress Cracking Resistance and Crystal Structure of

Polyethylene, Journal of Macromolecular Science, Part A. 51 (2014) 189–202. doi:10.1080/10601325.2014.871934.

[14] A. Adib, C. Domínguez, J. Rodríguez, C. Martín, R.A. García, The effect of microstructure on the slow crack growth resistance in polyethylene resins, Polymer Engineering & Science. 55 (2014) 1018–1023. doi:10.1002/pen.23970.

[15] M. Schilling, U. Niebergall, M. Böhning, Full notch creep test (FNCT) of PE-HD – Characterization and differentiation of brittle and ductile fracture behavior during environmental stress cracking (ESC), Polymer Testing. 64 (2017) 156–166. doi:10.1016/j.polymertesting.2017.09.043.

[16] L.M. Robeson, Environmental stress cracking: A review, Polymer Engineering & Science. 53 (2012) 453–467. doi:10.1002/pen.23284.

[17] Soares, João BP, R. F. Abbott, and J. D. Kim. "Environmental stress cracking resistance of

polyethylene: The use of CRYSTAF and SEC to establish structure–property

relationships." *Journal of Polymer Science Part B: Polymer Physics* 38.10 (2000): 1267-1275.

[18] ISO 16770 – Plastics – Determination of environmental stress cracking (ESC) of polyethylene – Full notch creep test (FNCT), 2004.

[19] ASTM D 5397 – Standard Test Method for Evaluation of Stress Crack Resistance of Polyolefin Geomembranes Using Notched Constant Tensile Load Test, 2007.

[20] ASTM International. ASTM F1473-16 Standard Test Method for Notch Tensile Test to Measure the Resistance to Slow Crack Growth of Polyethylene Pipes and Resins. West Conshohocken, PA: ASTM International, 2016. Web. 31 Mar 2017.

[21] ASTM International. ASTM D1693-15 Standard Test Method for Environmental Stress-Cracking of Ethylene Plastics. West Conshohocken, PA: ASTM International, 2015. Web. 31 Mar 2017.

[22] D. Huang, H. Zhou, L. Lin, Biodiesel: an Alternative to Conventional Fuel, Energy Procedia. 16 (2012) 1874–1885. doi:10.1016/j.egypro.2012.01.287.

[23] E. Richaud, Flaconnèche Bruno, J. Verdu, Biodiesel permeability in polyethylene, Polymer Testing. 31 (2012) 170–1076. doi:10.1063/1.4738433.

[24] M. Böhning, U. Niebergall, A. Adam, W. Stark, Influence of biodiesel sorption on temperature-dependent impact properties of polyethylene, Polymer Testing. 40 (2014) 133–142. doi:10.1016/j.polymertesting.2014.09.001.

[25] M.M. Maru, M.M. Lucchese, C. Legnani, W.G. Quirino, A. Balbo, I.B. Aranha, et al., Biodiesel compatibility with carbon steel and HDPE parts, Fuel Processing Technology. 90 (2009) 1175–1182. doi:10.1016/j.fuproc.2009.05.014.

[26] M. Böhning, U. Niebergall, A. Adam, W. Stark, Impact of biodiesel sorption on mechanical properties of polyethylene, Polymer Testing. 34 (2013) 17–24. doi:10.1016/j.polymertesting.2013.12.003.

[27] M. Böhning, U. Niebergall, M. Zanotto, V. Wachtendorf, Impact of biodiesel sorption on tensile properties of PE-HD for container applications, Polymer Testing. 50 (2016) 315–324. doi:10.1016/j.polymertesting.2016.01.025.

[28] M. Weltschev, J. Werner, M. Haufe, M. Heyer, Compatibility of High-Density Polyethylene Grades with Biofuels, Packaging Technology and Science. 27 (2013) 231–240. doi:10.1002/pts.2028.

[29] M. Thompson, B. Mu, C. Ewaschuk, Y. Cai, K. Oxby, J. Vlachopoulos, Long term storage of biodiesel/petrol diesel blends in polyethylene fuel tanks, Fuel. 108 (2013) 771–779. doi:10.1016/j.fuel.2013.02.040.

[30] A. Saad, F. Gomes, M. Thompson, Plasticizing effect of oxidized biodiesel on polyethylene observed by nondestructive method, Fuel. 252 (2019) 246–253. doi:10.1016/j.fuel.2019.04.122.

[31] F. Gomes, W. West, M. Thompson, Effects of annealing and swelling to initial plastic deformation of polyethylene probed by nonlinear ultrasonic guided waves, Polymer. 131 (2017) 160–168. doi:10.1016/j.polymer.2017.10.041.

[32] Y. Chen, Investigations of environmental stress cracking resistance of HDPE/EVA and LDPE/EVA blends, Journal of Applied Polymer Science. 131 (2013). doi:10.1002/app.39880.

[33] F. Gomes, M. Thompson, Analysis of Mullins effect in polyethylene using ultrasonic guided waves, Polymer Testing. 60 (2017) 351–356. doi:10.1016/j.polymertesting.2017.04.020.

[34] A. Krajenta, A. Rozanski, R. Idczak, Morphology and properties alterations in cavitating and non-cavitating high density polyethylene, Polymer. 103 (2016) 353–364. doi:10.1016/j.polymer.2016.09.068.

[35] C.J. Lissenden, Y. Liu, J.L. Rose, Use of non-linear ultrasonic guided waves for early damage detection, Insight - Non-Destructive Testing and Condition Monitoring. 57 (2015) 206–211. doi:10.1784/insi.2015.57.4.206.

[36] C.J. Lissenden, Y. Liu, G.W. Choi, X. Yao, Effect of Localized Microstructure Evolution on Higher Harmonic Generation of Guided Waves, Journal of Nondestructive Evaluation. 33 (2014) 178–186. doi:10.1007/s10921-014-0226-z.

[37] J.B.P. Soares, R.F. Abbott, J.D. Kim, Environmental stress cracking resistance of polyethylene: The use of CRYSTAF and SEC to establish structure–property relationships, Journal of Polymer Science Part B: Polymer Physics. 38 (2000) 1267. doi:10.1002/(sici)1099-0488(20000515)38:10<1267::aid-polb10>3.3.co;2-x.

[38] A. Lustiger, R. Markham, Importance of tie molecules in preventing polyethylene fracture under long-term loading conditions, Polymer. 24 (1983) 1647–1654. doi:10.1016/0032-3861(83)90187-8.

[39] R. Seguela, Critical review of the molecular topology of semicrystalline polymers: The origin and assessment of intercrystalline tie molecules and chain entanglements, Journal of Polymer Science Part B: Polymer Physics. 43 (2005) 1729–1748. doi:10.1002/polb.20414.

[40] P. Hittmair, R. Ullman, Environmental stress cracking of polyethylene, Journal of Applied Polymer Science. 6 (1962) 1–14. doi:10.1002/app.1962.070061901.

[41] A. Lustiger, R.D. Corneliussen, The role of crazes in the crack growth of polyethylene, Journal of Materials Science. 22 (1987) 2470–2476. doi:10.1007/bf01082132.

[42] A. Peterlin, Dependence of diffusive transport on morphology of crystalline polymers, Journal of Macromolecular Science, Part B. 11 (1975) 57–87. doi:10.1080/00222347508217855.

[43] A. Peterlin, Plastic deformation of polymers with fibrous structure, Colloid and Polymer Science. 253 (1975) 809–823. doi:10.1007/bf01452401.

[44] P. Withers, H. Bhadeshia, Residual stress. Part 1 – Measurement techniques, Materials Science and Technology. 17 (2001) 355–365. doi:10.1179/026708301101509980.

[45] P. Withers, H. Bhadeshia, Residual stress. Part 2 – Nature and origins, Materials Science and Technology. 17 (2001) 366–375. doi:10.1179/026708301101510087.

[46] S. Daniewicz, An elastic-plastic analytical model for predicting fatigue crack growth in arbitrary edge-cracked two-dimensional geometries with residual stress, International Journal of Fatigue. 16 (1994) 123–133. doi:10.1016/0142-1123(94)90102-3.

# Chapter

# 5. Conclusions and Future Work

The limited knowledge available on the compatibility of biodiesel with polyethylene has slowed down progress towards its independent use from fossil fuels to meet energy demands. More data on biodiesel related to its behavior with standard materials will ease risk concerns and speed up its implementation. The work presented investigates the compatibility of fresh and degraded biodiesel with different grades of polyethylene over a two-stage project using traditional test methods and a novel nondestructive test method based on ultrasonics. The purpose of the work was to improve material compatibility libraries for parts design involving exposure of polyethylene to this new biofuel.

Results from Stage One of the investigation revealed a plasticizing property of biodiesel on polyethylene. Gravimetric analysis of biodiesel in different grades of polyethylene displayed higher diffusivity coefficients (i.e. higher penetration rates) for the fuel in polyethylene samples of lower density. The sorption of biodiesel into polyethylene plasticized the samples thereby reducing their mechanical stiffness (Young’s Modulus), with the extent of plasticization dependent on the amount of fluid absorbed. Results from mechanical testing showed significantly higher plasticization efficiencies for biodiesel in comparison to toluene (a known plasticizing agent). Ultrasonic testing of the biodiesel and toluene plasticized samples revealed interesting evidence of differing modes of interaction (plasticization) with the semi-crystalline polymer structure between the two fluids. In comparison to toluene, immersion in biodiesel produced the opposite behavior in the third harmonic region for all tested grades. The increase in the positive ultrasonic parameter with exposure to toluene occurred in response to increasing internal stresses created by swelling. On the contrary, the increasingly negative ultrasonic parameter with exposure to biodiesel depicts a decrease in internal stresses and quite possibly suggests that the mode by which internal stresses build in a polymer is entirely different. The influence of oxidative degradation by biodiesel while contacting polyethylene was found to only affect the diffusion rate of the fuel, with no significant differences in the plasticizing ability when equivalent in concentration.

Results from Stage Two of the investigation explored the ability of biodiesel to act as an environmental stress cracking (ESC) agent, as suggested in Stage One by acoustic measurements. Polyethylene grades with a higher crystalline content and lower molecular weight (high MFI) were found to be prone to ESC by biodiesel, while samples with lower crystallinity and higher molecular weight (low MFI) were found to be more prone to only plasticization by biodiesel. Results from ultrasonic testing, gravimetric analysis, and infrared spectroscopy were used to illustrate the different modes of interaction by biodiesel with the different grades of polyethylene and propose a concentration-limited plasticization mechanism as the probable pathway for its ESC with polyethylene. Samples that cracked in biodiesel showed an initial decrease in the ultrasonic parameter (becoming more negative) till a minimum value, referred to as the “critical ultrasonic parameter threshold”, followed by an increase until crack initiation. The decrease in the ultrasonic parameter is associated with the relative decrease in internal stresses in response to localized absorption of biodiesel at the notch. The absorbed fuel plasticizes the polymer and weakens the tie chains in the amorphous region. The subsequent increase in the ultrasonic parameter arises in response to increasing internal stresses created by the penetrating molecules. The weakening of the tie chains at the notch, from localized plasticization by the absorbed biodiesel, along with the long-term low-level stresses applied to the face of the lamellae, from bending a sample, caused the tie chains to stretch and break until the number of tie molecules left is not sufficient to withstand the load applied, resulting in slippage or breakage of adjacent crystalline lamella and consequently failure of the sample. Visual inspection and infrared spectroscopy of the cracked samples revealed localized fluid absorption at the crack and notch site. On the contrary, samples that did not crack witnessed the same initial decline in the ultrasonic parameter with exposure to biodiesel but followed by a plateau at the end depicting that the biodiesel acted as a plasticizer for this polymer following the initial actions of a stress cracking agent, without actually cracking the sample Visual inspection and infrared spectroscopy of the samples that did not crack displayed bulk absorption of the fluid instead of localized absorption, resulting in softening of the polymer due to plasticization without cracking.

The safe use of biodiesel with polyethylene requires a great volume of data and research oriented towards the improvement of material compatibility libraries for parts design involving exposure of this relatively inert plastic to the new biofuel. Our investigations only analyze one type of biodiesel (tallow-based) with a limited number of polyethylene grades. Further experimental studies using the promising nondestructive ultrasonic testing technique should be carried out on using biodiesel from different sources on a larger number of polyethylene grades to extensively investigate the effects of the different properties of polyethylene (molecular weight, MFI, branching, crystallinity, etc.) on its compatibility with different sources biodiesel; data in the appendix gives a summary of all grades tested in this study. Data gathered from the proposed further investigations can help direct selection towards the best compatibility between different polyethylene grades and biodiesel from different sources by better understanding the different properties of the fuel and polyethylene that give rise to the different plasticization and ESC effects.

Finally, improvement and further development of the ultrasonic technique used can be done through analysis using different sensors. In this study, only one pair of transducers were used with vacuum grease as a coupling agent. The different ways of applying the vacuum grease between the sensors and the samples has brought about sources of errors that were minimized through repeats. As a result, further analysis should be done using alternative sensors, such as air-coupled and array sensors, that could improve performance by removing test barriers.

# Appendix

# A. Supplementary Material for Chapter 4

## A.1. Summary of all grades tested in biodiesel using the Bell Test

Regarding the initial discovery of biodiesel being a potential stress cracking agent, a large scale ESCR trial utilizing the Bell Test was organized using polyethylene grades of various properties. Table A.1 shows a summary of all grades tested using the Bell Test in pure biodiesel (B100), 10% biodiesel in water, and 10% biodiesel in petroleum diesel (B10).

**Table A.1.** Summary of all polyethylene grades tested using the Bell Test.

| **Reference Code** | **Type** | **Density** $(\frac{kg}{m^3})$ | **MFI** $(\frac{g}{10\ min})$ | **ESCR ($F_{50}$ hours)** | | | |
|---|---|---|---|---|---|---|---|
| | | | | **10% Igepal in water** | **Pure (B100) biodiesel** | **10% biodiesel in water** | **10% biodiesel in petroleum (B10) diesel** |
| HD 6908.19 | Homopolymer (HD) | 965 | 8.2 | 3 | 7 | N/A | N/A |
| HD 6605.70 | Hexene Copolymer (HD) | 948 | 5 | 20 | 13 | 13 | 13 |
| HD 6733.17 | Hexene Copolymer (HD) | 950 | 33 | 0 | N/A | N/A | N/A |
| HD 9830.02 | Bimodal Copolymer (HD) | 956 | 0.3 | 370 | >1000 | >1000 | N/A |

| | | | | | | | |
|---|---|---|---|---|---|---|---|
| LL 8460.29[1] | Hexene Copolymer (LL) | 938 | 3.3 | 60 | >1000 | >1000 | N/A |
| HD 8660.29[1] | Hexene Copolymer (HD) | 941 | 2 | 40 | >1000 | >1000 | >1000 |

### A.1.1. Polyethylene grades prone to environmental stress cracking in biodiesel

Only three polymer grades were found susceptible to ESC by biodiesel at 50 °C: HD 6908.19, HD 6605.70, and LA 080 (ref to Ch. 4). HD 6908.19 (ESCR = 3 hours) is a high density homopolymer with one of the lower ESCR ratings in the study. This can be due to the polymer's low molecular weight (high MFI - 8.2 g/10 min) and its high crystalline properties (69%). The low molecular weight of the polymer indicates lower availability of relatively long polymer chains for the formation of tie molecules (TMs)/chain entanglements spanning the interlamellar distance between crystallites. The high crystallinity provides the stiffness of the polymer and due to its bending, a large load is induced. This large load and low availability of TMs aggravates the acceleration of ESC, hence, reducing the ESCR of the polymer. HD 6908.19 cracked after approximately 7 hours in B100 biodiesel.

HD 6605.70 (ESCR = 20 hours) was tested in B100 biodiesel, 10% biodiesel in water, and B10 biodiesel. Samples in all three mediums saw cracking after approximately

---

[1]. W.T.J. West, 2017.

13 hours depicting comparable aggressiveness between the different environments (ref to Ch. 4). The lower yet relatively high crystalline content (58%) and low molecular weight (high MFI - 5.0 g/10 min) associated with this grade have made it susceptible to ESC by biodiesel but with more resistance than HD 6908.19. Inspection of both grades post cracking in biodiesel depicted distinct yellow staining around the crack and notch area.

The polymer grade HD 6733.17 failed to provide results with the Bell Test due to premature cracking of the samples prior to immersion in biodiesel. The narrow molecular weight hexane copolymer is the lowest ESCR rated sample with 0-hour rating. The narrow molecular weight distribution (MWD) possessed by this resin represents a lower possibility for formation of large molecules in the higher (molecular weight) end of the MWD spectrum. The absence of such large molecules diminishes many mechanical properties, including ESCR.

### A.1.2. Polyethylene grades resistant to environmental stress cracking in biodiesel

Polymer grades HD 8660.29 (ESCR = 40 hours), LL 8460.29 (ESCR = 60 hours), and HD 9830.02 (ESCR = 370 hours) were found to be largely immune to ESC by pure biodiesel. Samples in the Bell Test were left for over 1000 hours in biodiesel at 50 ℃ without cracking.

LL 8460.29 is a linear low density Hexene copolymer with a relatively high ESCR rating (60 hours). Samples in the B100 biodiesel and 10% biodiesel in water showed no signs of cracking, proving the superior ESCR of this grade in comparison to other high density grades. The low crystallinity (50%) and relatively high molecular weight (low

MFI - 2.0 g/10 min) polymer grade HD 8660.29 (ESCR = 40 hours) showed high resistance to ESC in B100 biodiesel, 10% biodiesel in water, and B10 biodiesel by not showing any signs of cracking despite being immersed for over1000 hours.

HD 9830.02 resin is a high density bimodal copolymer, therefore has a higher rated ESCR (ESCR = 370 hour). Samples in the Bell Test showed superior resistance to ESC after being immersed in B100 biodiesel and 10% biodiesel in water for more than 1,600 hours (67 days) without showing any signs of cracking or crazing. It is important to note that biodiesel's ability to stain the polymer provides a unique advantage of being able to visually detect its diffusion in polyethylene and thus, know where it is mostly concentrated in the sample (ref to Ch. 4). Unlike the grades that cracked in biodiesel, the polymer grades that did not crack had deeper yellow coloration on the whole sample and not just at the notch, depicting that whole body absorption occurred in these samples instead of localized fluid absorption and consequently, localized plasticization at the stress concentrated region (created by a pre-existing defect such as a notch) did not occur, which is necessary for ESC to happen.